Published in final edited form as:
*J Comp Neurol*. 2004 May 31; 473(3): 293–314. doi:10.1002/cne.20061.

# Chemoarchitectonic Subdivisions of the Songbird Septum and a Comparative Overview of Septum Chemical Anatomy in Jawed Vertebrates

**James L. Goodson***, **Andrew K. Evans**, and **Laura Lindberg**
*Psychology Department, University of California, San Diego, La Jolla, CA 92093 USA*

## Abstract

Available data demonstrate that the avian septal region shares a number of social behavior functions and neurochemical features in common with mammals. However, the structural and functional subdivisions of the avian septum remain largely unexplored. In order to delineate chemoarchitectural zones of the avian septum, we prepared a large dataset of double-, triple- and quadruple-labeled material in a variety of songbird species (finches and waxbills of the family Estrildidae and a limited number of emberizid sparrows) using antibodies against ten neuropeptides and enzymes. Ten septal zones were identified which are placed into lateral, medial, caudocentral and septohippocampal divisions, with the lateral and medial divisions each containing multiple zones. The distributions of numerous immunoreactive substances in the lateral septum closely match those of mammals (i.e., distributions of met-enkephalin, vasotocin, galanin, calcitonin gene-related peptide, tyrosine hydroxylase, vasoactive intestinal polypeptide, substance P, corticotropin-releasing factor, and neuropeptide Y), enabling detailed comparisons with numerous chemoarchitectonic zones of the mammalian lateral septum. Our septohippocampal and caudocentral divisions are topographically comparable to the mammalian septohippocampal and septofimbrial nuclei, respectively, although additional data will be required to establish homology. The present data also demonstrate the presence of a medial septal nucleus that is histochemically comparable to the medial septum of mammals. The avian medial septum is clearly defined by peptidergic markers and choline acetyltransferase immunoreactivity. These findings should provide a useful framework for functional and comparative studies, as they suggest that many features of the septum are highly conserved across vertebrate taxa.

### Keywords

lateral septum; medial septum; septofimbrial nucleus; evolution; bird; met-enkephalin; vasotocin; vasopressin; galanin; calcitonin gene-related peptide; tyrosine hydroxylase; vasoactive intestinal polypeptide; substance P; corticotropin-releasing factor; neuropeptide Y; choline acetyltransferase

The septum is a heterogeneous forebrain region that offers excellent opportunities for a variety of neuroethological studies, as it integrates a wide variety of spatial, social and stress-related processes. In all tetrapod vertebrates, the septum is strongly interconnected with the hippocampus (or proposed pallial equivalents; Krayniak and Siegel, 1978; Hoogland and Vermeulen-Vanderzee, 1993; Font et al., 1997; Risold and Swanson, 1997b; Font et al., 1998; Atoji et al., 2002; Westhoff and Roth, 2002) and also with a variety of structures in the brain's social behavior system (e.g., extended medial amygdala, preoptic area, anterior

*Correspondence: James L. Goodson, Psychology Department, 0109 (for courier, use 5212 McGill Hall), University of California, San Diego, La Jolla, CA 92093 USA, phone: (858) 822-4427, fax: (858) 534-7190, e-mail: jgoodson@ucsd.edu.

**Associate Editor:** Dr. John Rubenstein

hypothalamus, ventromedial hypothalamus and midbrain central gray; Krayniak and Siegel, 1978; Berk and Butler, 1981; Balthazart et al., 1994; Font et al., 1997; Risold and Swanson, 1997b; Font et al., 1998; Cheng et al., 1999). In both mammals and birds, the septum plays a role in the regulation of social behavior, particularly aggression and agonistic communication (Blanchard et al., 1977; Kollack-Walker et al., 1997; Goodson et al., 1999), and these processes are modulated by arginine vasotocin (AVT; homologue of mammalian arginine vasopressin, AVP; Koolhaas et al., 1990; Ferris et al., 1994; Goodson, 1998a,b; Goodson and Adkins-Regan, 1999). The AVT/AVP-immunoreactive (-ir) fibers in the lateral septum are testosterone-sensitive in many species (review: Goodson and Bass, 2001) and the lateral septum contains steroid hormone receptors (Martinez-Vargas et al., 1976; Morrell and Pfaff, 1978; Watson and Adkins-Regan, 1989; Simerly et al., 1990; Balthazart et al., 1992). Thus, the combined evidence suggests that the septum may integrate a variety of endocrine and contextual stimuli for the purpose of modulating complex behavior in a temporally, spatially and socially appropriate manner.

Birds offer exceptionally good opportunities for studies of these septal functions, as birds exceed other tetrapod vertebrate classes in their social and ecological diversity and excel in large-scale spatial navigation. Indeed, the available literatures on vertebrate social behavior, ecology and spatial navigation are heavily biased towards birds, particularly songbirds (see Alcock, 2001), thus birds offer the opportunity to study the septum in the context of well-characterized behaviors. However, the usefulness of such studies is severely limited by insufficient data on the anatomical organization of the avian septum. Given the functional, connectional and chemoarchitectural heterogeneity of the mammalian septum (Jakab and Leranth, 1995; Risold and Swanson, 1997a,b), it seems likely that 1) neurobehavioral studies of the avian septum will be of limited power and resolution until this large region is substantially parcellated, and 2) data generated in birds will be of limited utility for the generation of hypotheses in other vertebrates, particularly mammals, until an anatomical foundation is established that will allow for detailed comparisons between homologous subdivisions.

As described above, the avian septum and mammalian septum are comparable based upon gross anatomical and functional features. In addition, a number of histochemical features are likewise comparable (see Discussion) and available data suggest that the peptidergic constituents of the avian lateral septum are similar to those in mammals (Panzica et al., 1992, 1999; Aste et al., 1995, 1997; Bottjer and Alexander, 1995; Durand et al., 1998). However, no prior studies have been undertaken with the specific goal of delineating chemoarchitectonic zones of the avian septum and there is presently no consensus on even the largest septal subdivisions. For instance, different authors often depict the “medial septum” of birds in different topographical positions, or do not indicate its boundaries at all, and Roberts et al. (2002) recently suggested that the mediolateral organization of the avian septum may be fully reversed from that found in mammals. We will consider this latter argument more fully in the Discussion, but it should be noted that this organizational scheme is not consistent with hypotheses based upon the well-characterized peptidergic features of the avian “lateral septum” (particularly distributions of testosterone-sensitive AVT-ir fibers; see above) that suggest that the caudolateral region of the septum is equivalent between birds and mammals. Unfortunately, little clarification is available from connectional data, as very few tracings have been conducted from relevant hypothalamic nuclei and other forebrain structures (but see Berk and Butler, 1981; Balthazart et al., 1994; Atoji et al., 2002). In addition, while tracer injections into the septum indicate that the avian septum has grossly similar connections as the septum in mammals (Krayniak and Siegel, 1978), injections have not been made into restricted zones as might be suggested based upon current knowledge of septal organization (e.g., based upon more recent immunocytochemical studies).

This state of affairs contrasts strongly with that in mammals, particularly rats, in which multiple functional systems and 20 chemoarchitectonic zones have been described for the lateral septum alone (Risold and Swanson, 1997a,b). Thus, the present studies in songbirds were conducted in an effort to provide a definitive nomenclature and anatomical framework that will support detailed functional studies and meaningful comparisons with mammals. To this end, we have employed antibodies against ten neuropeptides and enzymes, including many substances that have been used by Risold and Swanson (1997a,b) to define the septal zones in rats. These antibodies were used to generate a variety of double-, triple- and quadruple-labeled material, thus providing clear evidence for the zonal distribution of substances.

## Methods

### Animals

Immunocytochemical material presented here was generated in five songbird species. Material was prepared explicitly for the present experiments in 35 zebra finches (Estrildidae: *Taeniopygia guttatta; n* = 15 males, 20 females), two male spice finches (Estrildidae: *Lonchura punctulata*) and five male song sparrows (Emberizidae: *Melospiza melodia*). Material that was generated as part of other experiments (in preparation) was also analyzed, including material from zebra finches (*n* = 6 males, 7 females), violet-eared waxbills (Estrildidae: *Uraeginthus granatina; n* = 7 males, 6 females), Angolan blue waxbills (Estrildidae: *Uraeginthus angolensis; n* = 7 males, 8 females), spice finches (*n* = 6 males, 6 females) and 21 male song sparrows.

Finches and waxbills used in the present studies were housed indoors on a 16L:8D photoperiod and were provided with finch seed mix, oyster shell and water *ad libitum*, with regular supplements of mealworms and greens. Violet-eared waxbills and Angolan blue waxbills were wild-caught in South Africa and spice finches were wild-caught from a feral population in Puerto Rico. These birds were maintained in captivity at least 4 mos prior to sacrifice. Song sparrows were wild-caught in San Diego County, CA and were perfused during the local breeding season (April-July). The zebra finches and song sparrows used in the present experiments were in reproductive condition; other species were sacrificed while in non-reproductive condition (gonads were fully regressed). Collections and procedures were conducted legally and humanely under all applicable federal and state permits and in compliance with all applicable institutional and federal guidelines.

### Primary antibodies and specifity

The following antibodies were employed in the present experiments: **Arginine vasopressin (AVP).** Guinea pig anti-AVP (Bachem; T-5048). **Calcitonin gene-related peptide (CGRP).** Guinea pig anti- CGRP (Bachem; T-5027). **Choline acetyltransferase (ChAT).** Rabbit anti- ChAT (a kind gift of Dr. Miles Epstein, University of Wisconsin). **Corticotropin releasing factor (CRF).** Guinea pig anti-CRF (Bachem; T-5007) and rabbit anti-CRF (Bachem; T-4036 and T-4037). **Galanin (GAL).** Guinea pig anti-GAL (Bachem; T-5034) and rabbit anti-GAL (Chemicon; AB1985). **Met-Enkephalin (ENK).** Mouse anti- ENK (Chemicon; MAB350). **Neuropeptide Y (NPY).** Rabbit anti-NPY (Bachem Immunochemicals, Torrance, CA; T-4070) and sheep anti-NPY (Chemicon, Temecula, CA; AB1583). **Substance P (SP).** Rabbit anti-SP (Chemicon; AB962). **Tyrosine hyrdroxylase (TH).** Sheep anti-TH (Novus Biologicals, Littelton, CO; NB 300-110). **Vasoactive intestinal polypeptide.** Guinea pig anti-VIP (Bachem; T-4030) and rabbit anti-VIP (Bachem; T-4246). All antibodies are polyclonal, with the exception of the anti-ENK, which is a mouse monoclonal. When secondary labeling was to be conducted in green or red color ranges (see below), a primary concentration of 1:1000 was used. When secondary labeling was to be conducted in blue or far-red color ranges, a primary concentration of 1:500 was used.

The specificities of all peptide antibodies were addressed by preadsorbing primary solutions overnight with 10-100 μM peptide (peptides purchased from Bachem and Phoenix Pharmaceuticals, Belmont, CA). Alternate tissue series were incubated with primary preadsorbed with peptide or saline. In all cases except anti-ENK, labeling was eliminated by incubation with 10 μM peptide. The ENK antibody is not specific to met-ENK and shows a weak reactivity to leu-ENK (manufacturer's data sheet). In our material, most labeling was eliminated by incubation with 10 μM met-ENK and was completely eliminated by incubation with 100 μM met-ENK. In contrast, 150 μM leu-ENK was required to eliminate labeling. The specificity of the TH antibody has been extensively addressed by the manufacturer (manufacturer's data sheet) and we performed no further assays. The rabbit anti-ChAT has been used extensively in birds (Medina and Reiner, 1994; Li and Sakaguchi, 1997; Roberts et al., 2002) and the specifity of this antibody has been fully detailed (Medina and Reiner, 1994).

**Material prepared explicitly for the present studies (see "Animals and housing" above)—**Labeling for all substances except ChAT was conducted in a minimum of four male and four female zebra finches, using one of two 40 μm coronal series. Some antibodies that were particularly informative (e.g., anti-TH and anti-NPY) were employed much more extensively to examine distributions relative to other substances. Anti-ChAT was employed in two male spice finches and two male song sparrows. Representative material using antibodies against TH, ENK, and NPY was also generated in a minimum of one song sparrow series each (see below for AVP and CRF).

**Additional material available for analysis—**Material from 21 song sparrows and 53 estrildid finches and waxbills (see "Animals and housing" above) was processed into three 40 μm series as part of other ongoing studies. Tissue from each finch and waxbill was labeled for TH, NPY, CRF, and AVP (at least one series for each antibody, including double-labeling for TH and NPY). One series from each song sparrow was labeled for AVP and CRF (separate series).

## Secondary antibodies

A wide range of secondary antibodies was employed in the present experiments. Given the variety of primary hosts (see above), we were able to generate numerous primary antibody line-ups for multi-labeling. Secondaries were selected for each line-up based upon the primary host species and issues of cross-reactivity. Secondary antibodies raised in donkey were used for line-ups that included sheep-derived primaries; secondaries raised in goat were used for all other labeling. In general, we sought to label as much material as possible using Alexa Fluors (Molecular Probes, Eugene, OR) as these fluorophores are stable for long periods of time. However, the cross-adsorptions available in Alexa Fluor-conjugated secondaries are not as extensive as those available in Cy -conjugated secondaries (Jackson ImmunoResearch, West Grove, PA) and we therefore made extensive use of Cy2 and Cy5 secondaries, as well as highly cross-adsorbed biotinylated secondaries from Jackson ImmunoResearch.

Fluorophores and secondary concentrations used for each color range are as follows. *Blue*: All labeling in the blue spectrum was conducted using a biotinylated secondary, 6 μl/ml, and streptavidin conjugated to Alexa Fluor 350, 6 μl/ml. *Green*: Cy2 or Alexa Fluor 488, 3 μl/ml. *Red*: Alexa Fluor 594, 3-5 μl/ml. *Far-red*: Cy5 and Alexa Fluor 680, 5-8 μl/ml. In cases where no blue labeling was conducted (which required biotinylation), biotin was occasionally employed in other color ranges. Regardless of the color range, biotinylation was conducted at a concentration of 3 μl/ml and this was followed by streptavidin conjugated to a fluorophore at the concentration given above. Finally, DAPI nuclear stain and/or a red fluorescent Nissl

stain (NeuroTrace 530/615; Molecular Probes) was employed to provide cytoarchitectural detail when the relevant color range was not being used for immunocytochemical labeling.

### Tissue Processing and Immunocytochemical Procedure

Subjects were deeply anesthetized by isoflurane vapor and intracardially perfused with 0.1M phosphate buffered saline (PBS; pH 7.4) followed by 4% paraformaldehyde. Brains were removed, post-fixed overnight and sunk in 30% sucrose for sectioning. Tissue was cut on a cryostat at thickness of 40 μm and collected into wells of 0.1M phosphate buffer (PB; pH 7.4) as free-floating sections.

Immunocytochemistry was performed as follows: 20 min in 10 mM sodium citrate (pH 9.5, ceramic well plates placed into a shallow water bath heated to 70° C); 20 min in PBS; 1 hr in PBS + 5.0% bovine serum albumin (BSA) + 0.3% triton-X; 16-42 h in primary antiserum diluted in PBS + 2.5% BSA + 0.3% triton-X + 0.05% sodium azide (performed at 4° C); two 30 min rinses in PBS; 2 h secondary in PBS + 2.5% BSA + 0.3% triton-X. All secondary labeling was conducted simultaneously except in cases where a biotinylated secondary was employed. In these cases, the tissue was incubated in biotinylated secondary for 1hr, rinsed for 30 min in PBS, and subsequently incubated in fluorophore-conjugated secondaries and streptavidin (see section above for concentrations). Sections were extensively washed in PBS and then transferred to PB prior to mounting. Tissue was mounted on slides and coverslipped.

A variety of mounting media were used, dependent upon the fluorphores being employed, as some media auto-fluoresce in the blue range and/or quench fluorophores in the far-red range. For material containing only green and/or red fluorophores, either Vectashield (Vector Labs, Burlingame, CA) or SlowFade Light (Molecular Probes) was used for coverslipping. Both of these media are available with DAPI nuclear stain. SlowFade Light, but not Vectashield, was found suitable for material labeled with far-red fluorophores. ProLong mounting medium (Molecular Probes) is suitable for all fluorophores but has a less desirable consistency; ProLong was thus used only for material containing Alexa Fluor 350 labeling (blue).

### Photomicroscopy

Photomicrographs were generated using a Zeiss Axioscop microscope equipped with a variety of single-band filters (ultraviolet, green, red and far-red filters from the ALPHA Vivid series, Omega Optical, Brattelboro, VT) and an Optronics Magnafire digital camera linked to a dual-processor Macintosh G4 computer. For each fluorophore, monochrome images were captured and contrast enhanced in Photoshop 5.5 for Macintosh prior to digital color merging and balancing. No re-touching of tissue flaws was performed. For the presentation of some material, one or more labeled substances were color merged in the camera software, selected and excised from the black background in Photoshop, and then superimposed on other color layers. This layered color montaging allowed greater color contrast in some material and allowed sparse or relatively weak label to be viewed in relation to more intense label. Pseudocoloring was also extensively used to enhance visibility and color contrast. In some cases, the photomicrographs of multilabeled material do not allow a full view of individual fiber systems. This is the case for SP, NPY and ENK, and we have therefore supplemented the color plates with single-label, grayscale photo series. All other substances are fully and accurately represented by the multilabel images. Photo panels were arranged and scaled in Adobe Illustrator 9.0, exported as Photoshop files and labeled in Photoshop.

## Results

Based upon patterns of overlap in the distributions of immunoreactive fibers, we recognized ten chemoarchitectonic zones. Table 1 lists these zones and their proposed rat equivalents, and

indicates the relative density of fibers immunoreactive for each substance in each of the avian zones. Substantial numbers of immunoreactive neurons were not observed for any of the substances examined, with the exception of ChAT, thus data regarding perikarya are considered only for ChAT. NPY- and TH-ir neurons were observed for some subjects, but these were very few in number (< 5 in any given subject). We chose to name the zones of the avian septum only after conducting detailed comparisons with rats, thus providing for a common or similar nomenclature when possible. Given that the rationale for nomenclature decisions was based largely upon comparative considerations, we will reserve full consideration of nomenclature for the Discussion. However, the descriptions below will be found more useful if placed in the context of our newly recognized subdivisions, so we will employ the new nomenclature for the presentation of the Results.

## Nuclei and regions associated with the septum

A few nuclei and regions that are closely associated with the septum bear mention in addition to the zones of the septum proper. Lateral septum organ (LSO). First is the LSO, a circumventricular organ that lies at the tip of the lateral ventricle at far-rostral levels of the septum. We will not consider this structure further, but readers can view the position of this structure in Figures 1A and 2A. Ventral forebrain islands (VFI). Immediately adjacent to the LSO is a previously unidentified region that we have called the VFI (Figs. 1A, 2A), a thin band of tissue that occupies a position strikingly similar to the islands of Calleja in mammals, which are associated with the olfactory tubercle. The VFI are distinct with some markers (e.g., NPY; Fig. 2A) and are chemoarchitecturally distinct from the adjacent LSO and LSc.vl.r. In addition to NPY, the VFI contain a modest density of SP-, CGRP- and GAL-ir fibers, and a low density of fibers immunoreactive for VIP, and ENK. Scattered ChAT-ir neurons are also occasionally observed in the ventromedial aspect of the VFI, adjacent to the septomesencephalic tract. The islands of Calleja in mammals exhibit similar chemoarchitectural features (Beckstead and Kersey, 1985; Fallon et al., 1983; Talbot et al., 1988), although there are differences in relative densities of various markers and data are not available for all substances examined here. Thus, while the present data suggest that the VFI may be most closely associated with the olfactory tubercle, satisfactory assignment of the VFI to any forebrain component must await further study. Diagonal band of Broca (DBB). There appears to be a clear consensus among authors as to the identity of the avian DB at rostral levels of septum, where the DBB extends ventrolaterally away from the midline of the septum, occupying a position immediately adjacent to the septomesencephalic tract (TrSM; Figs. 1A-B, 2A). In addition to this area, some authors recognize other DBB components more caudally, such as a horizontal limb on the dorsal surface of the anterior commissure and a vertical limb extending dorsally from the commissure into the ventromedial septum (e.g., Roberts et al., 2002). We have not attempted to characterize the avian DBB in the present study, but it should be noted that our internal band of the medial septum (MSib) may in fact be a component of the DBB rather than the MS proper. Additional data are required to resolve this issue. The MSib arises at rostral levels on the margin of the DBB (Fig. 1B), but as a distinct band, and occupies a position at commissural levels similar to the vertical limb of Roberts et al. (Figs. 1A, 2B, 3C, 4A, 5A, 5D, 7C). The MSib is considered more fully below. Nucleus of the pallial commissure (nPC) and commissural septal nucleus (CoS). We recognize the nPC and CoS as separate structures, although it appears that other authors may consider them to be a single entity, given the inconsistent use of nomenclature in the literature. The nPC lies within the cup of the pallial commissure (Fig. 1F-H) and is clearly visible with almost any staining or labeling. The nPC stains very densely for Nissl (Fig. 6B) and DAPI (Fig. 6D) and numerous immunoreactive substances distinguish its borders, either by completely filling the structure (NPY-, ENK-, SP-, CRF- and GAL-ir; Figs. 4B-C, 6A, 6E, 8B-C) or by rigidly skirting its margin (Figs. 3D, 6D). The nPC may be equivalent to portions of the posterior septal nuclei in mammals (triangular and septofimbrial nuclei), as addressed in the Discussion. The CoS arises on the lateral edge of the pallial

commissure (i.e., outside of the cup; Figs. 1F, 4C, 6A-B) and also appears quite dense in Nissl and DAPI stains (Fig. 6B, D). However, in contrast to the nPC, the CoS was virtually devoid of all labeling in our material and it therefore appears as a black “hole” in several of our photomicrographs (Fig. 3D, 4C-E, 6A, 6C). Progressing caudally from commissural levels, the position of the CoS moves laterally and eventually comes to lie underneath the tip of the lateral ventricle (Fig. 1F-I). At no level are the CoS and nPC contiguous.

## The septal zones

The line drawings in Figure 1 present an overview of the septal zones at multiple rostrocaudal levels, thus this figure may be used to add clarity to the topographical descriptions below. We recognize lateral septum (LS), medial septum (MS, including an internal band, MSib), septohippocampal (SH) and caudocentral septum (CcS) divisions. The LS and MS divisions are proposed to be homologous to the LS and MS of rats, respectively. The SH and CcS are topographically comparable to the septohippocampal nucleus and septofimbrial nucleus of rats, respectively, but additional data will be required to suggest homology (see Discussion). The LS is subdivided into rostral (LSr) and caudal (LSc) parts. In turn, we recognize medial and dorsolateral zones of the LSr (LSr.m and LSr.dl, respectively) and dorsal, lateral, ventral and ventrolateral zones of the LSc (LSc.d, LSc.l, LSc.v, and LSc.vl, respectively). As shown in Table 1 and Figure 1, some of these zones are further subdivided into regions that differ more modestly in their constituents. As discussed above, our nomenclature was developed to be consistent with mammals when possible. In this context, it should be noted that the rostral and caudal divisions (LSr and LSc) in birds are not positioned as predominantly rostral or caudal as is the case in mammals (i.e., the LSr and LSc are co-exstensive for throughout much of the septum). However, the avian LSr is more robust rostrally than caudally, and is not present at the most caudal levels of the septum (Fig. 1G-I). Also noteworthy is that the anterior commissure of songbirds is rostrocaudally centered within the length of the septum, which contrasts to a much more caudal placement in rodents, and the avian LSc appears to be concomitantly more expansive relative to the LSr.

**LSr.m and LSr.dl—**At rostral-most levels of the septum, the LSr occupies a central position in the septum and fully spans the septum mediolaterally (Figs. 1A-B, 2A, 3A-B). At progressively more caudal levels, the MSib and SH develop medial to the LSr (Fig. 1C) and the LSr subsequently maintains a dorsolateral position within the septum until disappearing at the level of the pallial commissure (Figs. 1D-F, 2B, 3C, 4A-B, 5A, 7C-D). The LSr.m is separated from the ventricular wall by the thin LSr.dl. These two zones of the LSr are easily distinguished from each other based on a few features: 1) TH-ir fibers are virtually absent in the LSr. dl but dense in the LSr.m (Figs. 2B, 3C, 5A), 2) peptidergic fibers are sparse in the LSr.m but dense in the LSr.dl (particularly NPY-, ENK-, and CGRP-ir fibers; Figs. 2B, 3C-D, 4A, 5A, 8A). The ENK-ir fibers in the LSr.dl represent the dorsal-most extension of the ENK-ir fibers which densely innervate the LS regions along the ventricular wall (Fig. 5A, 8A-B). Within the LSr.dl, this ENK-ir innervation is capped dorsally by a small and distinct CGRP-ir fiber plexus (compare Figs. 3C and 5A).

**LSc.d—**At rostral levels, the LSc.d can be distinguished from the LSr based largely upon TH-ir innervation, which is dense in the LSr.m and substantially more sparse in the LSc.d (Figs. 2A, 3A). In addition, peptidergic fibers coursing along the ventricular wall from the ventrolateral septum tend to reach their dorsal-most extent in the LSr.dl and are thus virtually absent in the LSc.d (Fig. 2B). NPY-ir fibers are also relatively sparse in the rostral aspect of the LSc.d (Fig. 2A). Progressing caudally, NPY-ir fibers streaming down from the hippocampus increase in density (Figs. 2B, 3A-F, 5A, 6A) and the TH-ir fibers of the LSc.d form a distinct band laterally and become absent medially (Figs. 2B, 3C, 5A). Thus, at mid-levels of the septum we distinguish a LSc.d.l and a LSc.d.m. This medial-lateral distinction

then disappears at far-caudal levels as the TH-ir fibers in the LSc.d become sparse. At all levels of the LSc.d, NPY-ir fibers characterize both medial and lateral aspects (see above).

**LSc.v—**The LSc.v is one of the most visibly distinct of the septal zones. Despite the fact that TH-ir fibers densely innervate surrounding septal zones, the TH-ir innervation of the LSc.v stands out as being particularly dense. TH-ir fiber nesting is much more extensive in the LSc.v than in the dorsally adjacent LSr.m and TH-ir fibers of the LSc.v are quite thick compared to fine-caliber fibers in the MS (Figs. 2A-B, 3A-D, 5A-D, 6A). Similarly, ENK-ir and VIP-ir processes are widespread in the LS, but extensively nest only in the LSc.v, primarily at middle and caudal levels (arrows, Fig. 8B-C). Peptidergic innervation of the LSc.v is largely absent at its rostral-most extent (i.e., at the level of Fig. 1A). The LSc.v occupies a position just medial to the elbow of the lateral ventricle at all levels except for the caudal-most extreme of the septum, where it is replaced by the CcS (Fig. 1)

**LSc.vl—**The LSc.vl contains the highest diversity of peptidergic fibers in the septum (see Table 1). Rostrally, where the septum is narrow and the MSib is not yet present, the LSc.vl forms a wide cup that cradles the ventral margin of the LSc.v and MS (Figs. 1A-B, 2A, 3A-B, 7A-B). Progressing caudally, the MS and MSib expand and the LSc.vl adopts a position more restricted to the ventrolateral LS (i.e., lateral to the MS; Figs. 1C-F, 2B, 3C, 4A-B, 5A-D, 7C-D, 8A). For much of its extent, the LSc.vl continues to cradle the ventrolateral aspect of the LSc.v and a dorsal extension of the LSc.vl forms a thin band that separates the LSc.v from the ventricular wall (e.g., Figs. 3D, 5A). Some peptidergic fibers in this dorsal band of the LSc.vl continue into the LSr.dl; these include ENK-ir and SP-ir fibers.

Most peptidergic fiber systems are present throughout the full rostrocaudal extent of the LSc.vl, or nearly so, although they tend to more densely innervate the caudal aspect of the LSc.vl; these include GAL, ENK, SP, VIP, and NPY. However, CGRP-ir fibers are particularly dense at rostral levels and almost absent at caudal levels (Fig. 3). This gradient is reversed for AVT. Hence, we distinguish an LSc.vl.r at rostral levels and a LSc.vl.c at caudal levels. The transition between these subdivisions is not distinct and the AVT-ir fiber distribution in the LSc.vl is increasingly variable at progressively more rostral levels. Finally, scattered CRF-ir fibers are present in the LSc.vl.c, appearing to arise predominantly from the lateral division of the bed nucleus of the stria terminalis.

**CcS and LSc.l—**Caudal to the anterior commissure, the LSc.vl expands medially, extending over the MS, which is beginning to disappear (Figs. 1F-G, 4A-B, 6B). As these fibers of the LSc.vl extend medially, two things occur: 1) The AVT- and GAL-fibers of the LSc.vl drop away from the ventricular wall, as do the more modest number of TH-ir fibers in this zone. The remaining paraventricular zone, the LSc.l, is thus characterized by an absence of these systems (Figs. 3D; 6A,C-D) and the presence of SP-, ENK-, VIP-, CRF-, and NPY-ir fibers (Figs. 4C-E, 6A,C, 7E, 8C). The density of CRF- and NPY-ir fibers is somewhat greater in the LSc.l than in the LSc.vl, whereas the density of VIP-ir fibers is somewhat less. The LSc.l is the most morphologically variable of the septal zones. In some animals, this zone forms a large peninsula that extends into the ventricle (see Figs. 4E, 6C for moderate cases), whereas in other subjects the LSc.l is present only as a thin band. 2) The peptidergic fibers of the LSc.vl are now joined by a larger number of CRF- and TH-ir fibers; this collection of fibers streams into the central septum, forming the CcS (Figs. 3D, 4C-F, 5A,C-E, 7E, 8C). There is no clear boundary between the CcS and the LSc.vl, but rather a graded shift in contributing systems. The CcS eventually expands to the full width of the septum as a finial cap, with only the LSc.d remaining dorsally (Figs. 1I, 4F, 6E).

**MS and MSib—**The MS and MSib arise as thin bands rostrally (Figs. 1B-C, 2A, 7A-B; 8A) and expand through commissural levels (Figs. 1C-E, 2B, 3C, 4A, 5A-D, 7C), after which they

shift ventrolaterally and disappear (Figs. 1F, 4B, 6B, 7D). The disappearance of the MS/MSib is accompanied by the expansion of the CcS, which appears as a caudal cap on the presumably subpallial zones of the septum (i.e., all except the LSc.d; see Puelles et al., 2000). At all levels, the MS and MSib are distinguished by exceptionally fine-caliber fibers, irrespective of the given substance being examined, providing a translucent appearance to label within the MS/MSib (see above). TH- and SP-ir fibers predominate throughout the MS whereas NPY- and VIP-ir fibers characterize the full extent of the MSib (Figs. 2B, 3C, 4A-B, 5A). A light ENK-ir innervation is also observed for the MSib (Fig. 8A). TH-ir fibers densely innervate the caudal half of the MSib as well; this innervation appears to originate as medial expansion of the TH-ir fiber plexus in the MS. This expansion of TH-ir fibers at commissural levels can be seen in Figure 5; panels A and B show TH-ir slightly more rostral to that shown in panels C and D (TH-ir is not present in the MSib in Fig. 5A-B). The entire MS/MSib complex is characterized by ChAT fibers and a large number of weakly labeled neurons are present caudally, particularly within the MS (Figs. 5D, 6B). The borders of the MS/MSib complex as defined by other substances precisely match the highest density of ChAT-ir label (Fig. 5D).

**SH—**The SH develops rostrally along the midline, just ventral to the LSc.d, and it expands until the level of the CcS (Figs. 1C-G). The position of the SH at progressively caudal levels can be seen in NPY-ir material, as in Fig. 4. At the level of the CcS, the SH begins to shift away from the midline (Figs. 3D, 4C-D, 6A) and flatten, finally forming a somewhat horizontal band along the dorsal margin of the CcS (Figs. 1H, 4E). The SH is characterized by SP-, NPY- and VIP-ir fibers, the latter two of which appear to originate in the hippocampus (Figs. 2B, 5A). The boundaries of the SH are not distinct, as a large territory in the midline septum appears to be occupied by fibers en passant, exiting the hippocampus (Figs. 2B, 5A, 6A). Importantly, the VIP- and SP-ir fibers appear to terminate in this zone rather than pass through, suggesting that this area should be considered a distinct division of the septum rather than a diffusely organized tract.

## Discussion

The regional distribution of most fiber systems described here for songbirds show extensive similarities with septal topography in mammals and other vertebrates, indicating that septal chemoarchitecture has been strongly conserved during tetrapod evolution. These comparative observations suggest that the avian septum is comprised of four major divisions - the lateral septum (LS), the medial septum (MS), the septohippocampal septum (SH) and the caudocentral septum (CcS), a division that caps the caudal aspect of the subpallial septum (for a description of the pallial/subpallial boundary, see Puelles et al., 2000). Based on the comparisons described below, we propose that the LS and MS divisions are homologous to the LS and MS of mammals, respectively. The SH and CcS are topographically comparable to the septohippocampal nucleus and septofimbrial nucleus (SFi) of rats, respectively, but additional data will be required to suggest homology. Comparisons of these major divisions with other vertebrate classes are presented in the next section. This is followed by detailed comparisons of the LS chemoarchitectonic zones in songbirds and rats, and by a practical overview of our findings in relation to other studies of the avian brain. We conclude with a brief discussion of functional considerations.

### Histochemical comparisons with the major septal divisions of other jawed vertebrates

Of the four major septal divisions here described, the LS is the most histochemically diverse, followed closely by the CcS, which appears as caudal expansion of the ventrolateral LS. Similarly, the mammalian LS and SFi are closely linked and the SFi may in fact be considered an extension of the LS (Risold and Swanson, 1997a,b). It should be noted that descriptions and/or illustrations of the caudal-most septum are absent in many of the papers cited below;

thus relatively few comparisons can be made between CcS histochemistry in songbirds and the caudal-most septum of other non-mammalian taxa. Somewhat more data are available on the caudal septum in mammals, where a distinct SFi and triangular nucleus are recognized. Similarly, comparisons of the avian SH can be made most readily with the septohippocampal nucleus of mammals, as equivalent zones have not been distinguished in other taxa.

Several substances exhibit fairly restricted distributions in the lateral aspect of the songbird septum (GAL, AVT, CGRP, ENK and CRF). These will be considered first in comparison to other tetrapod vertebrates, followed by an examination of substances that are more broadly distributed (NPY, VIP, SP and TH) and ChAT, which figures prominently in the identification of LS *vs.* MS divisions. We then present some comparative speculations on the posterior septal region and comparisons with basal forebrain regions in fishes, and conclude with a consideration of the present data relative to other chemoarchitectural features in birds.

**GAL—**Songbirds exhibit a GAL innervation along the lateral wall of the septum that is most dense ventrolaterally and more diffuse dorsally (present data). This topography is comparable to that described for the Japanese quail (*Coturnix japonica*, Azumaya and Tsutsui, 1996) and collared dove (*Streptopelia decaocto*, Dubbeldam et al., 1999) and is likewise similar to the distribution of GAL-ir fibers in the LS of anuran amphibians (*Rana esculenta* and *Xenopus laevis*, Lazar et al., 1991), turtles (*Mauremys scripta*, Jimenez et al., 1994), a variety of domestic mammals (sheep, Chaillou et al., 1999; rodents, Melander et al., 1986; Risold and Swanson, 1997a; Perez et al., 2001), and primates (*Cebus apella*, *Homo sapiens* and *Macaca mulatta*, Kordower and Mufson, 1990). Thus, the topography of GAL-ir fibers in the LS appears to have remained stable throughout tetrapod evolution. Indeed, comparisons of our data with the detailed line drawings for *Mauremys scripta* (Jimenez et al., 1994) suggest that the distribution of GAL-ir fibers in turtles and songbirds are virtually identical at all levels. In both cases, GAL-ir fibers form a ventral cup of fibers at rostral-most levels, a ventrolateral plexus at intermediate levels, and fill the full mediolateral span of the caudal-most septum. Dense GAL-ir fibers are likewise found for the mammalian SFi (see references above). In contrast, substantial species differences have been noted in the GAL-ir elements of the MS (e.g., Kordower and Mufson, 1990), including variation across avian species (Jozsa and Mess, 1993; Azumaya and Tsutsui, 1996; present study).

**AVP—**In birds, AVT/AVP-ir fibers exhibit a distribution that closely parallels that described above for GAL-ir fibers, with the exception that AVT/AVP-ir fibers are particularly sparse at rostral levels (Voorhuis and De Kloet, 1992; Aste et al., 1997, sPanzica et al., 1999; present study). AVT/AVP-ir fibers of the LS are also located in a predominantly caudal and ventrolateral position in a wide range of other vertebrate taxa, including a variety of reptiles (*Pseudemys scripta elegans* and *Python regius*, Smeets et al., 1990; *Gekko gecko*, Stoll and Voorn, 1985), anuran amphibians (*Rana catesbeiana*, Boyd et al., 1992; *Rana ridibunda* and *Xenopus laevis*, Gonzalez and Smeets, 1992a,b), and mammals (*Cavia porcellus*, Dubois-Dauphin et al., 1989; *Jaculus orientalis*, Lakhdar-Ghazal et al., 1995; *Meriones unguiculatus*, Crenshaw et al., 1992; *Microtus* sp., Wang et al., 1996; *Rattus* sp., De Vries et al., 1985; Risold and Swanson, 1997a). In many of these species, the AVT/AVP-ir innervation of the LS is testosterone-dependent and sexually dimorphic (review: Goodson and Bass, 2001), including birds (Voorhuis et al., 1988; Aste et al., 1997; Jurkevich et al., 2001; Panzica et al., 2001), providing additional support for the proposal that the AVT/AVP innervation of the ventrolateral LS is conserved across most tetrapod groups. However, this dense innervation has been substantially reduced in primates (*Callithrix jacchus*, Wang et al., 1997; *Homo sapiens*, Fliers et al., 1986; *Macaca fascicularis*, Caffe et al., 1989) and non-anuran amphibians (*Pleurodeles waltii*, Gonzalez and Smeets, 1992a; *Taricha granulosa*, Lowry et al., 1997; *Typhlonectes compressicauda*, Gonzalez and Smeets, 1997, *Typhlonectes natans*, Hilscher-Conklin et al., 1998). In the present material, we observed a modest number of AVP-ir

pericellular nests in the LS, a feature that has also been noted for other birds (e.g., Panzica et al., 1999) and rodents (e.g., Lakhdar-Ghazal et al., 1995). AVT/AVP-ir fibers within other septal areas show much more variation between species, particularly in the MS, which was virtually devoid of fibers in the present study. Finally, the current data revealed a dense AVP-ir fiber plexus in the CcS that is topographically comparable to a more modest innervation of the SFi in rodents (De Vries et al., 1985; Lakhdar-Ghazal et al., 1995).

**ENK—**Within the songbird LS, we observed a strong ENK-ir innervation which extended along the ventricular wall. This fiber plexus tapered off dorsally and did not enter the dorsal septum (LSc.d). A large number of pericellular baskets were found centrally located in this plexus. A few ENK-ir fibers were observed within the MS, mostly limited to the MSib. This distribution pattern is virtually identical to that described for all tetrapod species thus far examined; e.g., anuran amphibians (*Rana esculenta*, Merchenthaler et al., 1989), rats (Finley et al., 1981; Woodhams et al., 1983; Gall and Moore, 1984; Szeidemann et al., 1995; Risold and Swanson, 1997a), lizards (*Gekko gecko* and *Podarcis hispanica*, Russchen et al., 1987; Font et al., 1995) and a variety of birds (*Gallus domesticus*, Reiner et al., 1984a; *Melopsittacus undulates*, Durand et al., 1998; Roberts et al., 2002; *Taeniopygia guttata*, Bottjer and Alexander, 1995). While the density of ENK-ir fibers within the MS does vary somewhat across species, it is always substantially less dense than the fiber plexus along the ventricular wall. Finally, ENK-ir fibers densely innervate the songbird CcS (present study) and a similar case is found for the proposed SFi homologue in lizards (Font et al., 1995). However, ENK-ir within the mammalian SFi is largely limited to neurons and a dense ENK-ir fiber plexus is not present (Gall and Moore, 1984).

**CGRP—**Relatively few reports have provided detailed accounts of CGRP-ir within the septum. Sufficient data for comparisons are not available for amphibians, but are available for birds (*Coturnix japonica* and *Gallus domesticus*, Lanuza et al., 2000; *Melopsittacus undulates*, Durand et al., 2001; Roberts et al., 2002), a variety of reptiles (*Caiman crocodilus* and *Pseudemys scripta*, Brauth and Reiner, 1991; *Podarcis hispanica*, Martinez-Garcia et al., 2002) and rats (Sakanaka et al., 1985; Risold and Swanson, 1997a). In each case, CGRP-ir fibers are found along the ventricular wall of the LS. As with the peptidergic systems described above, CGRP-ir fibers are variably present in the MS at a much lower density than that found for the lateral wall. In both rats (Risold and Swanson, 1997a) and songbirds (present study), the fibers extending along the ventricular wall exhibit a distinct plexus dorsally that is juxtaposed to the dorsal-most extent of the ENK-ir innervation.

**CRF—**We observed a light CRF-ir innervation of the caudal ventrolateral LS in songbirds and a somewhat more substantial innervation of the CcS. No CRF-ir fibers were detected in the MS. Similarly, available data suggest that CRF-ir fibers in other species are typically located to the LS, but not the MS. Innervation of the LS is strong in snakes (*Bothrops jararaca*, Silveira et al., 2001; *Natrix maura*, Mancera et al., 1991) and at least a modest innervation is present in mammals (*Mesocricetus auratus*, Swanson et al., 1983; Sakanaka et al., 1988; Delville et al., 1992) and songbirds (*Sturnis vulgaris* and *Melospiza melodia*, Ball et al., 1989) but absent in a variety of ranid frogs (see Kozicz et al., 2002). In quail, CRF-ir fibers were observed within the MS, but not the LS (Panzica et al., 1986). CRF-ir fibers are not found for the posterior septal nuclei in mammals (Swanson et al., 1983).

**TH—**As found for songbirds (Bottjer, 1993; present study), TH-ir fibers in other tetrapods are widely distributed within the septum, with the most dense innervation being in the lateral aspect; e.g., rats (Gall and Moore, 1984; Risold and Swanson, 1997a), lizards (*Podarcis hispanica*, Font et al., 1995; *Gekko gecko*, Russchen et al., 1987), amphibians (*Typhlonectes compressicauda*, Gonzalez and Smeets Wilhelmus, 1994; *Rana perezi*, Sanchez-Camacho et

al., 2003), and non-passeriform birds (*Coturnix japonica*, Bailhache and Balthazart, 1993; *Columba livia*, Reiner et al., 1994; *Melopsittacus undulates*, Roberts et al., 2002). This lateral innervation is characterized by a distinct region containing coarse fibers and pericellular nests in all tetrapod classes, although within the Amphibia these are present only in gymnophionans (Gonzalez and Smeets, 1994). In songbirds and rats, the most prominent pericellular nesting overlaps the ENK-ir nests described above (Gall and Moore, 1984; Risold and Swanson, 1997a; present study). In contrast to the peptidergic systems described above, a substantial number of TH-ir fibers extend into the dorsal-most aspect of the LS in both songbirds and rats (Risold and Swanson, 1997a; present study). TH-ir fibers are also found within the mammalian SFi (Gall and Moore, 1984) and a proposed homologue in lizards (Font et al., 1995); these innervations are more modest than that observed for the CcS of songbirds (present data).

**NPY—**We observed a substantial number of NPY-ir fibers within all regions of the songbird septum except the MS proper, although a distinct NPY-ir fiber plexus does characterize the MSib. Despite being widespread, regional differences in density and/or axon caliber proved to be very useful in distinguishing the various septal nuclei, particularly the MSib, SH and LSc.d. Unfortunately, reports for other species typically describe NPY-ir fiber distributions for the whole brain and little specific information is provided on the septum, thus the present data can be compared to other groups only on a gross basis. In general, NPY-ir fibers are widely distributed in the vertebrate septum, encompassing both medial and lateral divisions; e.g., birds (*Coturnix japonica*, Aste et al., 1991; *Parus* sp., Gould et al., 2001), mammals (*Microcebus murinus*, Bons et al., 1990; *Spermophilus* sp., Reuss et al., 1990), reptiles (*Gallotia galloti*, Medina et al., 1992; *Podarcis hispanica*, Salom et al., 1994; *Chamaeleo chameleon*, Bennis et al., 2001), and amphibians (*Triturus cristatus*, Perroteau et al., 1988; *Xenopus laevis*, Tuinhof et al., 1994; *Typhlonectes natans*, Ebersole et al., 2001). An expansive NPY-ir innervation of the septum therefore appears to be a ubiquitous tetrapod feature, although there are large species differences in the presence and location of NPY-ir perikarya. We observed a small number of NPY-ir neurons in the ventrolateral aspect of the septum, but not in all subjects.

**VIP—**In the present material, VIP-ir fibers were concentrated in the subpallial LS and CcS, although a substantial fiber innervation was observed for the caudal-most LSc.d (presumably pallial; see Puelles et al., 2000). Pericellular nesting was observed in a region of the LS overlapping the area of densest nesting for TH- and ENK-ir fibers and VIP-ir fibers also clearly delineated the MSib and SH. A VIP-ir innervation of the LS has previously been documented in studies of birds (*Coturnix japonica*, Aste et al., 1995; *Taeniopygia guttata*, Bottjer and Alexander, 1995), reptiles (various species, Petko and Ihionvien, 1989; Hirunagi et al., 1993) and domestic rodents (Loren et al., 1979; Sims et al., 1980; Woodhams et al., 1983; Koves et al., 1991) and a light VIP-ir terminal field is reported for the MS in rats (Woodhams et al., 1983); VIP-ir fibers have not been described for the MS or medial wall of the septum in other species. In a pattern similar to that observed here, VIP-ir fibers in rats and mice are concentrated in the ventrolateral septum and also in the dorsal septum, but only at caudal levels (Loren et al., 1979).

**SP—**As shown here, SP-ir fibers are widespread within the songbird septum and are present within all divisions. However, SP-ir fibers are largely absent from the dorsal septum (LSc.d) except at caudal levels. As with other substances that exhibit broad distributions (e.g., NPY), variation in SP-ir fiber/plexus characteristics proved to be useful markers for delineating zones. In both songbirds (present study) and rats (Woodhams et al., 1983; Risold and Swanson, 1997a), SP-ir fibers form pericellular nests in a position overlapping the ENK- and TH-ir nests within the LS. We also observed nesting of the fine-caliber SP-ir fibers within the MS. Across a variety of species, SP-ir fibers most densely innervate the LS, with a more modest innervation of the MS; e.g., reptiles (*Chryemys picta* and *Pseudemys scripta*, Reiner et al., 1984b; *Gekko*

*gecko*, Russchen et al., 1987; *Podarcis hispanica*, Font et al., 1995; note that the MS is not recognized in *Podarcis*) and mammals (rats, Woodhams et al., 1983; Gall and Moore, 1984). However, SP-ir fibers have previously been reported only for the LS of birds (*Coturnix japonica*, Aste et al., 1995; *Parus* sp., Gould et al., 2001). In songbirds, we observed a SP-ir fibers within the CcS and a distinct terminal field in the SH; comparable observations are made for the SFi and septohippocampal nucleus of rats (Risold and Swanson, 1997a).

**ChAT and delineation of the MS and LS—**Based on examinations of cholinergic systems in a variety of birds (Medina and Reiner, 1994; Li and Sakaguchi, 1997; Roberts et al., 2002; present study), it is evident that the avian septum contains only a modest component of the basal forebrain cholinergic neurons. This is a substantial difference between birds and mammals (Mesulam et al., 1983; Brauer et al., 1999), but might be anticipated based on experiments in reptiles, particularly *Podarcis hispanica*, the only diapsid (and only non-mammal) for which a substantial amount of data are available on septal subdivisions, chemoarchitecture (Font et al., 1995) and connectivity (Font et al., 1997, 1998). An equivalent of the mammalian MS is not recognized for *Podarcis*; rather, MS-like features appear to be restricted to associated areas of the basal forebrain (diagonal band nucleus and bed nucleus of the medial forebrain bundle). In fact, although a substantial number of cholinergic neurons are present in the MS of anuran amphibians (Marin et al., 1997), this population of cells is greatly reduced or virtually absent in urodeles (Marin et al., 1997), turtles (Mufson et al., 1984; Powers and Reiner, 1993), crocodilians (Brauth et al., 1985) and a lizards (Hoogland and Vermeulen-VanderZee, 1990; Medina et al., 1993). Nonetheless, a large population of cholinergic neurons is present in the basal forebrain of all these species.

In pigeons (*Columba livia*, Medina and Reiner, 1994) and budgerigars (*Melopsittacus undulates*, Roberts et al., 2002), virtually no ChAT-ir neurons were observed in the position of the MS using the same anti-chicken ChAT employed here (neurons were located primarily adjacent to the pallial commissure in CoS and/or diagonal band), whereas a substantial population of small ChAT-ir perikarya was observed in the LS. These observations led to quite different conclusions by the respective authors. Roberts et al. (2002) suggest that the mediolateral organization of the avian septum may be fully reversed from that found in mammals, based not only upon the relative concentrations of cholinergic neurons, but also upon the observation that the MS is the major septal target of projections from the avian medial amygdala (nucleus taeniae; Cheng et al., 1999). In contrast, Medina et al. (1994) conclude that the ChAT-ir neurons of the LS are not related to the basal forebrain cholinergic system, because the LS does not project to cortical-like areas in pigeons, whereas those of the CoS/ventromedial septum do project to the hippocampus (e.g., Casini et al., 1986, but see Atoji et al., 2002). This observation weakens the hypothesis of Roberts et al. (2002) and the present findings clearly support the view of Medina et al. (1994). In addition, the projections of nucleus taeniae (Cheng et al., 1999) are not completely inconsistent with the conclusions of Medina et al. (1994), as terminal fields are observed in the ventrolateral LS in addition to the MS. Finally, it should be noted that novel populations of cholinergic neurons in the LS are not restricted to birds, but have also been observed in raccoons (*Procyon lotor*; Brauer et al., 1999) and gymnophionans (*Dermophis mexicanus*; Gonzalez et al., 2002).

In the present material, we found a relative density of ChAT-ir neurons within the septum that is different from that observed in these other avian taxa. While we did observe a few immunopositive neurons in the LS, the majority of ChAT-ir neurons within the septum were concentrated in the MS, primarily at caudal levels. ChAT-ir fibers were most dense within the MS as well. This topography is consistent with photomicrographs presented for zebra finches by Li and Sakaguchi (1997). Thus, substantial variation is present across avian species in the MS cholinergic cell group, with the songbirds representing a condition that is most similar to

anuran amphibians (Marin et al., 1997) and mammals (Mesulam et al., 1983; Brauer et al., 1999).

In weighing the full spectrum of data presented here and by others, we believe that the case for homology between the avian LS and the LS of other tetrapods is solidly supported, and that the case for homology between the avian MS and the MS of other vertebrates is also somewhat compelling. The chemoarchitectural details presented in the above sub-sections provide strong evidence that many details of LS organization have been strongly conserved during vertebrate evolution. Limited connectional data are consistent with this view, most notably the fact that the hippocampus exhibits a topographic projection to the LS in both mammals (Risold and Swanson, 1997b) and birds (Atoji et al., 2002). Data for the MS are less clear, as substantial variation exists across species in the chemical anatomy of this area (see above). Nonetheless, a “medial septum” that contains at least a modest number of ChAT-ir neurons associated with the basal forebrain cholinergic cell group is present the ventromedial septum of most tetrapod groups. Likewise, limited data suggest comparable connectivity of the MS in mammals and birds. In mammals, the MS projects heavily upon the hippocampus, whereas only a minor hippocampal projection arises in the LS (Jakab and Leranth, 1995). Despite some discrepancies, the combined evidence from pigeons suggests a comparable pattern (Casini et al., 1986; Atoji et al., 2002). Detailed connectional studies on the avian septum would be useful in solidifying these points, and are essential for any substantive discussion of the posterior septum, as addressed below.

**Additional comments on the SH and posterior septum—**The posterior septum of mammals is comprised of the SFi and triangular nucleus (Jakab and Leranth, 1995; Risold and Swanson, 1997a,b). Non-mammalian equivalents of these nuclei have not been identified except for *Podarcis* (Font et al., 1995, 1997, 1998), in which the midline septal division exhibits connectional and topographical features similar to the posterior septal nuclei of mammals. Thus, the midline nuclei in *Podarcis* may be equivalent as a field to the posterior septum of mammals, although a one-to-one correspondence of their constituent nuclei is not evident. The avian nPC occupies a position comparable to the midline division of *Podarcis* and the triangular nucleus of mammals, and the position of the CcS within the caudal septum is very similar to that of the mammalian SFi. However, there are major species differences in the histochemistry of these regions. The midline septal division of *Podarcis* and the avian nPC/CcS both exhibit ENK- and TH-ir fibers (Font et al., 1995; present study; additional comparative data are not available). However, unlike the nPC/CcS, neither the mammalian SFi nor triangular nucleus exhibits a strong TH-, ENK- or SP-ir terminal field, although it is worth noting that these systems are in fact present at low density (Risold and Swanson, 1997a). A similar observation is made for AVP-ir fibers (De Vries et al., 1985).

The case for comparisons between the septohippocampal nucleus of mammals and the SH of songbirds is much more compelling, despite the limited lines of evidence. First, the topography of these areas is both unusual and strikingly similar. Rostrally, the SH is positioned on the dorsal midline, and the SH begins to shift away from the midline at post-commissural levels in both songbirds and rats. The SH then flattens dorsoventrally and comes to lie over the dorsal margin of the SFi/CcS. As already described, the SFi/CcS caps the caudal end of the subpallial septum (as defined by Puelles et al., 2000) in both mammals and birds. Secondly, of seven substances which were examined both here and by Risold and Swanson (1997a), only SP is present in the SH of rats and songbirds. All other substances are not present in either taxa. Additional substances that characterize the avian SH (VIP and NPY) were not examined in the studies of Risold and Swanson and insufficient data are available from other mammalian studies to allow comparisons.

**Comparisons with teleost and cartilaginous fishes—**Identification of the septum homologue in teleosts is complicated by the everted development of the telencephalon. However, the ventral nucleus of the ventral telencephalon (Vv) shares multiple characteristics in common with the lateral septum and associated basal forebrain structures of tetrapods (Northcutt, 1995) and tract tracings from a number of structures support the comparison of Vv to the septum of tetrapods (Wong, 1997; Goodson and Bass, 2002). A variety of substances that characterize the septum of songbirds and other tetrapods (see above) are likewise found within the teleost Vv, including fibers immunoreactive for NPY, CRF, SP, TH, and ENK (Hornby et al., 1987; Reiner and Northcutt, 1992; Vecino et al., 1992; Vecino and Sharma, 1992; Zupanc et al., 1999; Pepels et al., 2002) as well as cholinergic neurons (Brantley and Bass, 1988). The drawings of Batten et al. (1990) also suggest the presence of CGRP-, VIP- and GAL-ir terminal fields in the vicinity of Vv (not labeled). The septal region of chondrichthyans has been little explored, but does contain ChAT-, ENK-, TH- and SP-ir fibers, but no ChAT-ir perikarya (Northcutt et al., 1988; Anadon et al., 2000).

**Relation to other chemoarchitectural features in birds—**As addressed above, the distributions of numerous substances have been extensively described for the avian septum (e.g., AVT, VIP, and ENK). In addition to these, much data are available on the distributions of other substances, particularly gonadotropin releasing hormone (GnRH) and nicotinamide adenine dinucleotide phosphate-diaphorase (NADPH-diaphorase). As described above, the chemical anatomy of the MS is far less conserved than that of the LS, and this is observation applies to the distribution of NADPH-diaphorase-ir neurons as well. An intensely stained cluster of NADPH-diaphorase-ir perikarya distinguishes the MS and nPC of quail (MS position equivalent to that describe here; (Panzica et al., 1994), but the MS population is absent in *Columba livia* (Atoji et al., 2001) and *Melopsittacus undulates* (Cozzi et al., 1997). In contrast, GnRH neurons are consistently observed within the LS/caudal septum of both songbirds (Saldanha et al., 1994) and non-songbirds (Kuenzel and Blahser, 1991; Panzica et al., 1992; van Gils et al., 1993). The distribution of GnRH-ir neurons described for the septum closely matches the position of our LSc.vl, LSc.l and CcS. This topographical assignment is corroborated by double-label data that show a close correspondence between GnRH-ir neurons and fibers immunoreactive for VIP and CRF (Teruyama and Beck, 2001; Wang and Millam, 1999). The CRF double-label data are particularly informative, as CRF-ir fibers in the present study were located only to the LSc.vl, LSc.l and CcS.

## Detailed comparisons of LS chemoarchitectonic zones in songbirds and mammals

Based on a large body of data from immunocytochemical and *in situ* hybridization studies, Risold and Swanson (1997a) divide the rat LS into rostral, caudal and ventral divisions (LSr, LSc and LSv, respectively). These authors employed antisera against ten substances, seven of which were examined here (ENK, CRF, CGRP, SP, AVP, GAL and TH). The major divisions are comprised of multiple “zones,” which are in turn divided into “regions,” some of which are further divided into sub-regions (“domains”). Despite the complexity that is inherent in such a detailed organizational scheme, the authors generated a relatively straightforward nomenclature based upon topographical criteria. For instance, the medial zone of the LSr is designated as the LSr.m; the ventrolateral region of that zone is designated as the LSr.m.vl; and the lateral domain of that region is designated as the LSr.m.vl.l.

The criteria for placing rat zones into the three major parts (LSr, LSc and LSv) relate primarily to the distributions of mRNA expression, which are absent from our current dataset on songbirds. However, we were able to identify equivalents of most zones based upon immunocytochemical criteria. Thus, in order to provide a nomenclature for the avian LS that can be readily compared to the rat nomenclature of Risold and Swanson (1997a), we combined most zones which are comparable to the rat LSr zones into an avian LSr, and place most zones

which are comparable to the rat LSc into an avian LSc. Minor exceptions and related rationale are addressed below. In both rats and songbirds, the LSr and LSc are not exclusively rostral or caudal; rather, these areas are present at virtually all levels of the septum, but tend to be most expansive either rostrally or caudally. Absent from our organization scheme is an LSv, which consists of only one zone in mammals. Features of the LSv appear to be incorporated into a component of our LSc (see below).

**LSr—**Risold and Swanson (1997a) recognize three zones within the LSr – the LSr.m, LSr.dl, and the LSr.vl. Two of these zones are apparent in birds, most clearly the LSr.dl. In rats, the LSr.dl is characterized by a distinct plexus of CGRP-ir fibers that caps the dorsal-most extent of the ENK-ir fiber plexus in the LSr.dl.l. SP-ir fibers are also found in the rat LSr.dl. As discussed above, the ENK-ir plexus of the LS is virtually invariant across tetrapods in its topography. As in rats, these ENK-ir fibers in songbirds are capped dorsally by a distinct plexus of CGRP-ir fibers that overlaps the position of SP-ir fibers. Positioned medial to the rat LSr.dl is the LSr.m, which contains dense TH-ir fibers but is virtually devoid of peptidergic inputs. Again, a topographically similar and histochemically identical zone is observed for songbirds and is therefore designated as the LSr.m. The LSr.vl of rats is not strongly characterized by any of the antisera employed with the exception of one region (LSr.vl.v) that does contain an SP-ir input. We were unable to identify an obviously comparable zone in birds (but see below for speculations on the rostral portion of the songbird LSc.vl). In both rats and songbirds, the LSr is most expansive rostral to the anterior commissure, although a caudal remnant of the songbird LSr.m is present to the level of the pallial commissure.

**LSc and LSv—**The LSc of rats is divided into dorsal and ventral zones, the LSc.d and LSc.v. The LSc.d is topographically comparable to the dorsal septum (LSd) as recognized in earlier organizational schemes (Jakab and Leranth, 1995; Risold and Swanson, 1997b) and this area appears to correspond to the pallial septum as delineated by gene expression data in chicks and mice (Puelles et al., 2000). The histochemistry of this area is likewise comparable between songbirds and rats: In each case, the LSc.d labels negatively for most substances, but does exhibit a TH-ir plexus in its lateral aspect (LSc.d.l in both rats and songbirds). In songbirds, the LSc.d also exhibits a strong NPY-ir input. While NPY immunoreactivity was not examined by Risold and Swanson (1997a), NPY-ir fibers are indeed found within the dorsal septum of mammals (e.g., Reuss et al., 1990).

The LSc.v of rats is divided into medial, intermediate and lateral regions, the LSc.v.m, LSc.v.i and LSc.v.l. The LSc.v.i is a small area situated between the other two regions and is not distinguished by any immunohistochemical criteria. We did not identify this region in songbirds, and the proposed avian homologues of the rat LSc.v.m and the LSc.v.l are therefore closely juxtaposed with no interposing area. The LSc.v.m of rats is characterized by the most dense TH-ir fiber nesting within the septum, SP-ir fibers and nests, and ENK-ir pericellular nests (ENK-ir nests within this region are not explicitly addressed by the authors, but shown in Fig. 8 of Risold and Swanson, 1997a). A histochemically and topographically comparable area is present in songbirds that is also contains particularly distinct TH-ir pericellular nests. We have designated this zone as the LSc.v.

Ventrolateral to the rat LSc.v.m (our LSc.v) lies the LSc.v.l, a region that characterized by a strong innervation by AVP- and GAL-ir fibers. Again, a topographically and histochemically comparable area is observed in birds that we designate the LSc.vl, or more specifically, the LSc.vl.c (the rostral component of the LSc.vl, the LSc.vl.r, will be addressed below). As described in the previous section, many tetrapods exhibit a steroid-sensitive AVT/AVP-ir fiber innervation of the caudal ventrolateral septum (Goodson and Bass, 2001), thus supporting the proposal that the LSc.vl.c of birds and the LSc.v.l of rats are homologous. However, this area in birds may also incorporate a neuronal population that is equivalent to the LSv of rats. The

rat LSv is closely juxtaposed to the LSc.v.l and is primarily characterized by SP-ir fibers, androgen receptors (also present in the rat LSc.v.l) and estrogen receptors. While we did not observe an SP-ir terminal field that is distinct from other peptidergic systems in songbirds, other studies in birds have demonstrated the presence of steroid receptors (Arnold et al., 1976; Martinez-Vargas et al., 1976; Balthazart et al., 1989; Watson and Adkins-Regan, 1989; Balthazart et al., 1998) in a position matching that of the songbird LSc.vl.c, which does contain SP-ir fibers. As shown in Table 1, we therefore propose that the songbird LSc.vl.c contains neuronal populations homologous to both the rat LSc.v.l and the LSv.

The avian LSc.vl is bordered by a relatively small periventricular zone that we have designated the LSc.l. Unlike the LSc.vl, the LSc.l is largely devoid of AVP- and GAL-ir fibers, but densely innervated by NPY- and ENK-ir fibers. While NPY-ir was not examined by Risold and Swanson (1997a,b) for rats, those authors do show a small periventricular zone of the LSr (LSr.dl.l.v) that is adjacent to the LSc.v.l and characterized primariliy by a strong ENK-ir input. While we consider it likely that the avian LSc.l is equivalent to the rat LSr.dl.l.v, we have chosen to place this small area into the LSc rather than the LSr, as its position in birds (more caudal than in rats) and a variety immunocytochemical markers suggest that it is closely linked to the LSc.vl (see Table 1).

Our last area of the LS to consider, and the most difficult, is the songbird LSc.vl.r. As shown in Table 1, this area is histochemically comparable to the songbird LSc.vl.c (and thus the rat LSc.v.l), but is only very sparsely innervated by AVP-ir fibers and instead contains a dense CGRP-ir fiber plexus. This rostral extension of the LSc.vl extends more medially, forming a cup along the ventral margin of the septum (see Figs. 1A-B, 2A). In rats, the LSc.v.l is bounded rostroventrally by the LSr.vl.v (which also cups the ventral margin of the septum) and rostrodorsally by the LSr.dl.m. As noted above, we did not identify an equivalent of the rat LSr.vl.v, which is characterized by SP-ir inputs, and while we did identify an equivalent of the LSr.dl.l, we did not identify an equivalent of the LSr.dl.m, which is characterized by CGRP- and SP-ir fibers. Given that 1) the LSc.v.l of rats is rostrally juxtaposed to the LSr.vl.v and the LSr.dl.m, and 2) the songbird LSc.vl.r contains peptidergic inputs comparable to all three of these regions, we propose that the songbird LSc.vl.r is homologous in part to the LSc.v.l, LSr.vl.v and LSr.dl.m of rats.

## Practical application of the avian septum nomenclature

While the present data suggest that the avian septum has a complex organization, the positions of the various zones and divisions can be readily identified using a modest number of markers (as few as one; see below). Unfortunately, Nissl staining is not a particularly useful tool for this purpose, as the cytoarchitecture and chemoarchitecture of the septum do not closely correspond. A similar case is found for rats (Risold and Swanson, 1997a, b) and connectional features of the rat LS correspond well to chemoarchitectural features but not to cytoarchitecture. Thus, in the context of other studies (e.g., immediate early gene experiments; Goodson et al., 2003) we have made extensive use of immunocytochemical labeling to identify the septal zones. Two points are particulary important in this regard. First, the positions of the major divisions and LS zones can be visualized (or accurately calculated) using only one or two antibodies. TH labeling is particularly informative, as the various TH-positive zones (MS/MSib, LSc.d.l, LSr.m, LSc.v and CcS) are readily distinguished from each other based on spatial segregation and/or axonal features (caliber, density, varicosities and nesting). The other major zones and divisions typically border these TH-positive areas, or are in fact outlined by them. For our immediate early gene experiments, we have used one of three tissue series for immunocytochemical markers, typically NPY and TH, which clearly delineate all zones. A second important point is that the positions of the zones are relatively consistent across individuals of the same species. Using TH- and NPY-ir material from a small number of finches

and waxbills, we have generated a series of polygon templates for specific rostrocaudal levels that can be superimposed upon photomicrographs from any other finch or waxbill to delineate the septal zones. Given that tissue from all of the subjects was labeled for TH and NPY, we have been able to verify that a small number of reference series can in fact be usefully and accurately employed to calculate the position of the septal zones in other subjects. This method is most accurate at rostrocaudal levels where zones are not in rapid transition.

### Conclusions and functional speculations

The present data demonstrate that songbirds possess MS and LS divisions that are similar in many ways to the MS and LS of other vertebrates. In general, the histochemistry of the MS varies much more across taxa than does the LS. The MS appears to be completely absent in some lizards (Font et al., 1998), and the cholinergic neurons of the MS are relatively few in reptiles and non-oscine birds (i.e., non-songbirds) relative to the number found in anuran amphibians and mammals (see above). We found that songbirds possess a cholinergic neuron population that is of intermediate size. As in mammals (Jakab and Leranth, 1995), this population may give rise to hippocampal projections (Casini et al., 1986) and modulate learning and memory functions. In contrast to the MS, the LS exhibits many histochemical features that are quite similar across vertebrate taxa, including fish. Thus, the septal equivalents in fish contain many of the same substances as the LS of tetrapods, and within the tetrapods, the LS is chemoarchitectonically organized in a strongly conserved manner. Given this, we were able to recognize multiple LS zones in songbirds that are likely homologous to LS zones in rats (Risold and Swanson, 1997a). Detailed tract tracings of the songbird septum remain to be conducted, but the present results suggest that as in mammals (Risold and Swanson, 1997b), we may expect to find substantial heterogeneity in the connections of the LS zones, forming an anatomical bases for the differential involvement of the LS zones in arousal, anxiety, defense, and a number of physiological functions. Consistent with this, we have found that immediate early gene induction within the LS zones varies in response to non-social stress (handling) and social stress (territorial challenge), with the zones exhibiting different response profiles (Goodson et al., 2003).

## Acknowledgements

Grant sponsor: National Institutes of Health grant number R01 MH62656

## References

Alcock, J. Animal Behavior: An Evolutionary Approach. Sunderland, MA: Sinauer Associates; 2001.

Anadon R, Molist P, Rodriguez-Moldes I, Lopez JM, Quintela I, Cervino MC, Barja P, Gonzalez A. Distribution of choline acetyltransferase immunoreactivity in the brain of an elasmobranch, the lesser spotted dogfish (*Scyliorhinus canicula*). J Comp Neurol 2000;420:139–170. [PubMed: 10753304]

Arnold AP, Nottebohm F, Pfaff DW. Hormone concentrating cells in vocal control and other areas of the zebra finch (*Poephila guttata*). J Comp Neurol 1976;165:487–512. [PubMed: 1262541]

Aste N, Viglietti-Panzica C, Fasolo A, Andreone C, Vaudry H, Pelletier G, Panzica GC. Localization of neuropeptide Y-immunoreactive cells and fibres in the brain of the Japanese quail. Cell Tissue Res 1991;265:219–230. [PubMed: 1934027]

Aste N, Viglietti-Panzica C, Fasolo A, Panzica GC. Mapping of neurochemical markers in quail central nervous system: VIP- and SP-like immunoreactivity. J Chem Neuroanat 1995;8:87–102. [PubMed: 7541207]

Aste N, Viglietti-Panzica C, Balthazart J, Panzica GC. Testosterone modulation of peptidergic pathways in the septo-preoptic region of male Japanese quail. Poult Avian Biol Rev 1997;8:77–93.

Atoji Y, Yamamoto Y, Suzuki Y. Distribution of NADPH diaphorase-containing neurons in the pigeon central nervous system. J Chem Neuroanat 2001;21(1):1–22. [PubMed: 11173217]

Atoji Y, Wild JM, Yamamoto Y, Suzuki Y. Intratelencephalic connections of the hippocampus in pigeons (*Columba livia*). J Comp Neurol 2002;447:177–199. [PubMed: 11977120]

Azumaya Y, Tsutsui K. Localization of galanin and its binding sites in the quail brain. Brain Res 1996;727:187–195. [PubMed: 8842397]

Bailhache T, Balthazart J. The catecholaminergic system of the quail brain: Immunocytochemical studies of dopamine beta-hydroxylase and tyrosine hydroxylase. J Comp Neurol 1993;329:230–256. [PubMed: 8095939]

Ball GF, Faris PL, Wingfield JC. Immunohistochemical localization of corticotropin-releasing factor in selected brain areas of the European starling (*Sturnus vulgaris*) and the song sparrow (*Melospiza melodia*). Cell Tissue Res 1989;257:155–161. [PubMed: 2787697]

Balthazart J, Dupiereux V, Aste N, Viglietti-Panzica C, Barrese M, Panzica GC. Afferent and efferent connections of the sexually dimorphic medial preoptic nucleus of the male quail revealed by in vitro transport of DiI. Cell Tissue Res 1994;276:455–475. [PubMed: 8062340]

Balthazart J, Foidart A, Houbart M, Prins GS, Ball GF. Distribution of androgen receptor-immunoreactive cells in the quail forebrain and their relationship with aromatase immunoreactivity. J Neurobiol 1998;35:323–340. [PubMed: 9622014]

Balthazart J, Foidart A, Wilson EM, Ball GF. Immunocytochemical localization of androgen receptors in the male songbird and quail brain. J Comp Neurol 1992;317:407–420. [PubMed: 1578004]

Balthazart J, Gahr M, Surlemont C. Distribution of estrogen receptors in the brain of the Japanese quail: An immunocytochemical study. Brain Res 1989;501:205–214. [PubMed: 2819436]

Batten TFC, Cambre ML, Moons L, Vandesande F. Comparative distribution of neuropeptide-immunoreactive systems in the brain of the green molly *Poecilia latipinna*. J Comp Neurol 1990;302:893–919. [PubMed: 2081820]

Beckstead RM, Kersey KS. Immunohistochemical demonstration of differential substance P-, met-enkephalin-, and glutamic-acid-decarboxylase-containing cell body and axon distributions in the corpus striatum of the cat. J Comp Neurol 1985;232:481–498. [PubMed: 2579980]

Bennis M, Ba m'hamed S, Rio JP, Le Cren D, Reperant J, Ward R. The distribution of NPY-like immunoreactivity in the chameleon brain. Anat Embryol 2001;203:121–128. [PubMed: 11218058]

Berk ML, Butler AB. Efferent projections of the medial preoptic nucleus and medial hypothalamus in the pigeon. J Comp Neurol 1981;203:379–399. [PubMed: 6274919]

Blanchard DC, Blanchard RJ, Takahashi LK, Takahashi T. Septal lesions and aggressive behavior. Behav Biol 1977;21:157–161. [PubMed: 561603]

Bons N, Mestre N, Petter A, Danger JM, Pelletier G, Vaudry H. Localization and characterization of neuropeptide Y in the brain of *Microcebus murinus* (Primate, Lemurian). J Comp Neurol 1990;298:343–361. [PubMed: 2212108]

Bottjer SW. The distribution of tyrosine hydroxylase immunoreactivity in the brains of male and female zebra finches. J Neurobiol 1993;24:51–69. [PubMed: 8093477]

Bottjer SW, Alexander G. Localization of met-enkephalin and vasoactive intestinal polypeptide in the brains of male zebra finches. Brain Behav Evol 1995;45:153–177. [PubMed: 7796094]

Boyd SK, Tyler CJ, De Vries GJ. Sexual dimorphism in the vasotocin system of the bullfrog *Rana catesbeiana*. J Comp Neurol 1992;325:313–325. [PubMed: 1460117]

Brantley RK, Bass AH. Cholinergic neurons in the brain of a teleost fish (*Porichthys notatus*) located with a monoclonal antibody to choline acetyltransferase. J Comp Neurol 1988;275:87–105. [PubMed: 3170792]

Brauer K, Holzer M, Bruckner G, Tremere L, Rasmusson DD, Poethke R, Arendt T, Hartig W. Two distinct populations of cholinergic neurons in the septum of raccoon (*Procyon lotor*): Evidence for a separate subset in the lateral septum. J Comp Neurol 1999;412:112–122. [PubMed: 10440713]

Brauth SE, Kitt CA, Price DL, Wainer BH. Cholinergic neurons in the telencephalon of the reptile *Caiman crocodilus*. Neurosci Lett 1985;58:235–240. [PubMed: 4047484]

Brauth SE, Reiner A. Calcitonin-gene related peptide is an evolutionarily conserved marker within the amniote thalamo-telencephalic auditory pathway. J Comp Neurol 1991;313:227–239. [PubMed: 1765582]

Caffe AR, Van Ryen PC, Vand Der Woude TP, Van Leeuwen FW. Vasopressin and oxytocin systems in the brain and upper spinal cord of *Macaca fascicularis*. J Comp Neurol 1989;287:302–325. [PubMed: 2778107]

Casini G, Bingman VP, Bagnoli P. Connections of the pigeon dorsomedial forebrain studied with WGA-HRP and 3H-proline. J Comp Neurol 1986;245:454–470. [PubMed: 2422224]

Chaillou E, Tramu G, Tillet Y. Distribution of galanin immunoreactivity in the sheep diencephalon. J Chem Neuroanat 1999;17:129–146. [PubMed: 10609862]

Cheng M, Chaiken M, Zuo M, Miller H. Nucleus taenia of the amygdala of birds: Anatomical and functional studies in ring doves (*Streptopelia risoria*) and European starlings (*Sturnus vulgaris*). Brain Behav Evol 1999;53:243–270. [PubMed: 10473902]

Cozzi B, Massa R, Panzica GC. The NADPH-diaphorase-containing system in the brain of the budgerigar (Melopsittacus undulatus). Cell Tissue Res 1997;287(1):101–112. [PubMed: 9011384]

Crenshaw BJ, De Vries GJ, Yahr P. Vasopressin innervation of sexually dimorphic structures of the gerbil forebrain under various hormonal conditions. J Comp Neurol 1992;322:589–598. [PubMed: 1401252]

De Vries GJ, Buijs RM, van Leeuwen FW, Caffe AR, Swaab DF. The vasopressinergic innervation of the brain in normal and castrated rats. J Comp Neurol 1985;233:236–254. [PubMed: 3882778]

Delville Y, Stires C, Ferris CF. Distribution of corticotropin-releasing hormone immunoreactivity in golden hamster brain. Brain Res Bull 1992;29:681–684. [PubMed: 1422865]

Dubbeldam JL, van Ommen MH, den Boer-Visser AM. Immunohistochemical characterization of forebrain areas in the collared dove (*Streptopelia decaocto*). Eur J Morphol 1999;37:134–138. [PubMed: 10342445]

Dubois-Dauphin M, Tribollet E, Dreifuss JJ. Distribution of neurohypophysial peptides in the guinea-pig brain i. an immunocytochemical study of the vasopressin-related glycopeptide. Brain Res 1989;496:45–65. [PubMed: 2804653]

Durand SE, Brauth SE, Liang W. Calcitonin gene-related peptide immunoreactive cells and fibers in forebrain vocal and auditory nuclei of the budgerigar (*Melopsittacus undulatus*). Brain Behav Evol 2001;58:61–79. [PubMed: 11805374]

Durand SE, Liang W, Brauth SE. Methionine enkephalin immunoreactivity in the brain of the budgerigar (*Melopsittacus undulatus*): Similarities and differences with respect to oscine songbirds. J Comp Neurol 1998;393:145–168. [PubMed: 9548694]

Ebersole TJ, Conlon JM, Goetz FW, Boyd SK. Characterization and distribution of neuropeptide Y in the brain of a caecilian amphibian. Peptides 2001;22:325–334. [PubMed: 11287086]

Fallon JH, Loughlin SE, Ribak CE. The islands of Calleja complex of rat basal forebrain. III. Histochemical evidence for a striatopallidal system. J Comp Neurol 1983;218:91–120. [PubMed: 6136533]

Ferris CF, Delville Y, Irvin RW, Potegal M. Septo-hypothalamic organization of a stereotyped behavior controlled by vasopressin in golden hamsters. Physiol Behav 1994;55:755–759. [PubMed: 8190806]

Finley JC, Maderdrut JL, Petrusz P. The immunocytochemical localization of enkephalin in the central nervous system of the rat. J Comp Neurol 1981;198:541–565. [PubMed: 7019273]

Fliers E, Guldenaar SEF, Wal NVD, Swaab DF. Extrahypothalamic vasopressin and oxytocin in the human brain presence of vasopressin cells in the bed nucleus of the stria terminalis. Brain Res 1986;375:363–367. [PubMed: 3524745]

Font C, Hoogland Piet V, Van Der Zee Eefke V, Perez CJ, Martinez Garcia F. The septal complex of the telencephalon of the lizard *Podarcis hispanica*: I. Chemoarchitectonical organization. Journal of Comparative Neurology 1995;359:117–130. [PubMed: 8557841]

Font C, Lanuza E, Martinez-Marcos A, Hoogland PV, Martinez-Garcia F. Septal complex of the telencephalon of lizards: III. Efferent connections and general discussion. J Comp Neurol 1998;401:525–548. [PubMed: 9826276]

Font C, Martinez-Marcos A, Lanuza E, Hoogland PV, Martinez-Garcia F. Septal complex of the telencephalon of the lizard *Podarcis hispanica*: II. Afferent connections. J Comp Neurol 1997;383:489–511. [PubMed: 9208995]

Gall C, Moore RY. Distribution of enkephalin, substance P, tyrosine hydroxylase, and 5-hydroxytryptamine immunoreactivity in the septal region of the rat. J Comp Neurol 1984;225:212–227. [PubMed: 6202728]

Gonzalez A, Lopez JM, Sanchez-Camacho C, Marin O. Localization of choline acetyltransferase (ChAT) immunoreactivity in the brain of a caecilian amphibian, *Dermophis mexicanus* (Amphibia: Gymnophiona). J Comp Neurol 2002;448:249–267. [PubMed: 12115707]

Gonzalez A, Smeets WJAJ. Distribution of tyrosine hydroxylase immunoreactivity in the brain of *Typhlonectes compressicauda* (Amphibia, Gymnophiona): Further assessment of primitive and derived traits of amphibian catecholamine systems. J Chem Neuroanat 1994;8:19–32. [PubMed: 7893418]

Gonzalez A, Smeets WJAJ. Comparative analysis of the vasotocinergic and mesotocinergic cells and fibers in the brain of two amphibians, the anuran *Rana ridibunda* and the urodele *Pleurodeles waltlii*. J Comp Neurol 1992a;315:53–73. [PubMed: 1541723]

Gonzalez A, Smeets WJAJ. Distribution of vasotocin and mesotocin-like immunoreactivities in the brain of the south african clawed frog *Xenopus laevis*. J Chem Neuroanat 1992b;5:465–479. [PubMed: 1476666]

Gonzalez A, Smeets WJAJ. Distribution of vasotocin- and mesotocin-like immunoreactivities in the brain of *Typhlonectes compressicauda* (Amphibia, Gymnophiona): Further assessment of primitive and derived traits of amphibian neuropeptidergic systems. Cell Tissue Res 1997;287:305–314. [PubMed: 8995201]

Goodson JL. Territorial aggression and dawn song are modulated by septal vasotocin and vasoactive intestinal polypeptide in male field sparrows (*Spizella pusilla*). Horm Behav 1998a;34:67–77. [PubMed: 9735230]

Goodson JL. Vasotocin and vasoactive intestinal polypeptide modulate aggression in a territorial songbird, the violet-eared waxbill (Estrildidae: *Uraeginthus granatina*). Gen Comp Endocrinol 1998b;111:233–244. [PubMed: 9679095]

Goodson JL, Adkins-Regan E. Effect of intraseptal vasotocin and vasoactive intestinal polypeptide infusions on courtship song and aggression in the male zebra finch (*Taeniopygia guttata*). J Neuroendocrinol 1999;11:19–25. [PubMed: 9918225]

Goodson JL, Bass AH. Social behavior functions and related anatomical characteristics of vasotocin/vasopressin systems in vertebrates. Brain Res Rev 2001;35:246–265. [PubMed: 11423156]

Goodson JL, Bass AH. Vocal-acoustic circuitry and descending vocal pathways in teleost fish: Convergence with terrestrial vertebrates reveals conserved traits. J Comp Neurol 2002;448:298–322. [PubMed: 12115710]

Goodson JL, Eibach R, Sakata J, Adkins-Regan E. Effect of septal lesions on male song and aggression in the colonial zebra finch (*Taeniopygia guttata*) and the territorial field sparrow (*Spizella pusilla*). Behav Brain Res 1999;98:167–180. [PubMed: 10210532]

Goodson JL, Evans AK, Lindberg L. The septal region of songbirds: Chemoarchitectonic zones and activation by social stimuli. Horm Behav 2003;44:52.

Gould KL, Newman SW, Tricomi EM, DeVoogd TJ. The distribution of substance P and neuropeptide Y in four songbird species: a comparison of food-storing and non-storing birds. Brain Res 2001;918:80–95. [PubMed: 11684045]

Hilscher-Conklin C, Conlon JM, Boyd SK. Identification and localization of neurohypophysial peptides in the brain of a caecilian amphibian, *Typhlonectes natans* (Amphibia: Gymnophiona). J Comp Neurol 1998;394:139–151. [PubMed: 9552122]

Hirunagi K, Rommel E, Oksche A, Korf HW. Vasoactive intestinal peptide-immunoreactive cerebrospinal fluid- contacting neurons in the reptilian lateral septum/nucleus accumbens. Cell and Tissue Research 1993;274:79–90. [PubMed: 8242714]

Hoogland PV, Vermeulen-VanderZee E. Distribution of choline acetyltransferase immunoreactivity in the telencephalon of the lizard *Gekko gecko*. Brain Behav Evol 1990;36:378–390. [PubMed: 2073575]

Hoogland PV, Vermeulen-Vanderzee E. Medial cortex of the lizard *Gekko gecko*: A hodological study with emphasis on regional specialization. J Comp Neurol 1993;331:326–338. [PubMed: 8514912]

Hornby PJ, Piekut DT, Demski LS. Localization of immunoreactive tyrosine hydroxylase in the goldfish brain. J Comp Neurol 1987;261:1–14. [PubMed: 2887592]

Jakab, RL.; Leranth, C. Septum. In: Paxinos, G., editor. The Rat Nervous System. San Diego: Academic Press; 1995. p. 405-442.

Jimenez AJ, Mancera JM, Perez-Figares JM, Fernandez-Llebrez P. Distribution of galanin-like immunoreactivity in the brain of the turtle *Mauremys caspica*. J Comp Neurol 1994;349:73–84. [PubMed: 7531723]

Jozsa R, Mess B. Galanin-like immunoreactivity in the chicken brain. Cell Tissue Res 1993;273:391–399. [PubMed: 7689938]

Jurkevich A, Grossmann R, Balthazart J, Viglietti-Panzica C. Gender-related changes in the avian vasotocin system during ontogeny. Microsc Res Tech 2001;55:27–36. [PubMed: 11596147]

Kollack-Walker S, Watson SJ, Akil H. Social stress in hamsters: Defeat activates specific neurocircuits within the brain. J Neurosci 1997;17:8842–8855. [PubMed: 9348352]

Koolhaas, JM.; Moor, E.; Hiemstra, Y.; Bohus, B. The testosterone-dependent vasopressinergic neurons in the medial amygdala and lateral septum: involvement in social behavior of male rats. In: Jaard, S.; Jamison, R., editors. Vasopressin. Paris: INSERM/Libbey; 1990. p. 213-220.

Kordower JH, Mufson EJ. Galanin-like immunoreactivity within the primate basal forebrain: Differential staining patterns between humans and monkeys. J Comp Neurol 1990;294:281–292. [PubMed: 1692044]

Koves K, Arimura A, Gorcs TG, Somogyvari-Vigh A. Comparative distribution of immunoreactive pituitary adenylate cyclase activating polypeptide and vasoactive intestinal polypeptide in rat forebrain. Neuroendocrinology 1991;54:159–169. [PubMed: 1766552]

Kozicz T, Arimura A, Maderdrut JL, Lazar G. Distribution of urocortin-like immunoreactivity in the central nervous system of the frog *Rana esculenta*. J Comp Neurol 2002;453:185–198. [PubMed: 12373783]

Krayniak PF, Siegel A. Efferent connections of the septal area in the pigeon. Brain Behav Evol 1978;15:389–404.

Kuenzel WJ, Blahser S. The distribution of gonadotropin-releasing hormone (GnRH) neurons and fibers throughout the chick brain (Gallus domesticus). Cell Tissue Res 1991;264(3):481–495. [PubMed: 1868520]

Lakhdar-Ghazal N, Dubois Dauphin M, Hermes MLHJ, Buijs RM, Bengelloun WA, Pevet P. Vasopressin in the brain of a desert hibernator, the Jerboa (*Jaculus orientalis*): Presence of sexual dimorphism and seasonal variation. J Comp Neurol 1995;358:499–517. [PubMed: 7593745]

Lanuza E, Davies DC, Landete JM, Novejarque A, Martinez-Garcia F. Distribution of CGRP-like immunoreactivity in the chick and quail brain. J Comp Neurol 2000;421:515–532. [PubMed: 10842211]

Lazar GY, Liposits ZS, Toth P, Trasti SL, Maderdrut JL, Merchenthaler I. Distribution of galanin-like immunoreactivity in the brain of *Rana esculenta* and *Xenopus laevis*. J Comp Neurol 1991;310:45–67. [PubMed: 1719037]

Li R, Sakaguchi H. Cholinergic innervation of the song control nuclei by the ventral paleostriatum in the zebra finch: A double-labeling study with retrograde fluorescent tracers and choline acetyltransferase immunohistochemistry. Brain Res 1997;763:239–246. [PubMed: 9296565]

Loren I, Emson PC, Fahrenkrug J, Bjorkland A, Alumets J, Hakanson R, Sundler F. Distribution of vasoactive intestinal polypeptide in mouse and rat brain. Neuroscience 1979;4:1953–1976. [PubMed: 394023]

Lowry CA, Richardson CF, Zoeller TR, Miller LJ, Muske LE, Moore FL. Neuroanatomical distribution of vasotocin in a urodele amphibian (*Taricha granulosa*) revealed by immunohistochemical and in situ hybridization techniques. J Comp Neurol 1997;385:43–70. [PubMed: 9268116]

Mancera JM, Lopez Avalos MD, Perez-Figares JM, Fernandez-Llebrez P. The distribution of corticotropin-releasing factor immunoreactive neurons and nerve fibers in the brain of the snake *Natrix maura*: Coexistence with arginine vasotocin and mesotocin. Cell Tissue Res 1991;264:539–548. [PubMed: 1868522]

Marin O, Smeets WJ, Gonzalez A. Distribution of choline acetyltransferase immunoreactivity in the brain of anuran (*Rana perezi*, *Xenopus laevis*) and urodele (*Pleurodeles waltl*) amphibians. J Comp Neurol 1997;382:499–534. [PubMed: 9184996]

Martinez-Garcia F, Novejarque A, Landete JM, Moncho-Bogani J, Lanuza E. Distribution of calcitonin gene-related peptide-like immunoreactivity in the brain of the lizard *Podarcis hispanica*. J Comp Neurol 2002;447:99–113. [PubMed: 11977114]

Martinez-Vargas MC, Stumpf WE, Sar M. Anatomical distribution of estrogen target cells in the avian CNS: A comparison with the mammalian CNS. J Comp Neurol 1976;167:83–103. [PubMed: 1270623]

Medina L, Marti E, Artero C, Fasolo A, Puelles L. Distribution of neuropeptide Y-like immunoreactivity in the brain of the lizard *Gallotia galloti*. J Comp Neurol 1992;319:387–405. [PubMed: 1602050]

Medina L, Reiner A. Distribution of choline acetyltransferase immunoreactivity in the pigeon brain. J Comp Neurol 1994;342:497–537. [PubMed: 8040363]

Medina L, Smeets WJ, Hoogland PV, Puelles L. Distribution of choline acetyltransferase immunoreactivity in the brain of the lizard *Gallotia galloti*. J Comp Neurol 1993;331:261–285. [PubMed: 8509502]

Melander T, Hokfelt T, Rokaeus A. Distribution of galaninlike immunoreactivity in the rat central nervous system. J Comp Neurol 1986;248:475–517. [PubMed: 2424949]

Merchenthaler I, Lazar G, Maderdrut JL. Distribution of proenkephalin-derived peptides in the brain of *Rana esculenta*. J Comp Neurol 1989;281:23–39. [PubMed: 2784450]

Mesulam MM, Mufson EJ, Wainer BH, Levey AI. Central cholinergic pathways in the rat: An overview based on an alternative nomenclature (Ch1-Ch6). Neuroscience 1983;10:1185–1201. [PubMed: 6320048]

Morrell JI, Pfaff DW. A neuroendocrine approach to brain function: Localization of sex steroid concentrating cells in vertebrate brains. Am Zool 1978;18:447–460.

Mufson EJ, Desan PH, Mesulam MM, Wainer BH, Levey AI. Choline acetyltransferase-like immunoreactivity in the forebrain of the red-eared pond turtle (*Pseudemys scripta elegans*). Brain Res 1984;323:103–108. [PubMed: 6395936]

Northcutt RG. The forebrain of gnathostomes: In search of a morphotype. Brain Behav Evol 1995;46:275–318. [PubMed: 8564468]

Northcutt RG, Reiner A, Karten HJ. Immunohistochemical study of the telencephalon of the spiny dogfish, *Squalus acanthias*. J Comp Neurol 1988;277:250–267. [PubMed: 2466059]

Panzica GC, Arevalo R, Sanchez F, Alonso JR, Aste N, Viglietti-Panzica C, Aijon J, Vazquez R. Topographical distribution of reduced nicotinamide adenine dinucleotide phosphate-diaphorase in the brain of the Japanese quail. J Comp Neurol 1994;342:97–114. [PubMed: 8207130]

Panzica GC, Aste N, Castagna C, Viglietti-Panzica C, Balthazart J. Steroid-induced plasticity in the sexually dimorphic vasotocinergic innervation of the avian brain: Behavioral implications. Brain Res Rev 2001;37:178–200. [PubMed: 11744086]

Panzica GC, Aste N, Viglietti-Panzica C, Fasolo A. Neuronal circuits controlling quail sexual behaviour: Chemical neuroanatomy of the septo-preoptic region. Poult Sci Rev 1992;4:249–259.

Panzica GC, Plumari L, Garcia-Ojeda E, Deviche P. Central vasotocin-immunoreactive system in a male passerine bird (*Junco hyemalis*). J Comp Neurol 1999;409:105–117. [PubMed: 10363714]

Panzica GC, Viglietti-Panzica C, Fasolo A, Vandesande F. CRF-like immunoreactive system in the quail brain. J Hirnforsch 1986;27:539–547. [PubMed: 3540107]

Pepels PP, Meek J, Wendelaar Bonga SE, Balm PH. Distribution and quantification of corticotropin-releasing hormone (CRH) in the brain of the teleost fish *Oreochromis mossambicus* (tilapia). J Comp Neurol 2002;453:247–268. [PubMed: 12378586]

Perez SE, Wynick D, Steiner RA, Mufson EJ. Distribution of galaninergic immunoreactivity in the brain of the mouse. J Comp Neurol 2001;434:158–185. [PubMed: 11331523]

Perroteau I, Danger JM, Biffo S, Pelletier G, Vaudry H, Fasolo A. Distribution and characterization of neuropeptide Y-like immunoreactivity in the brain of the crested newt. J Comp Neurol 1988;275:309–325. [PubMed: 3225341]

Petko M, Ihionvien M. Distribution of substance P, vasoactive intestinal polypeptide and serotonin immunoreactive structures in the central nervous system of the lizard, *Lacerta agilis*. J Hirnforsch 1989;30:415–423. [PubMed: 2477439]

Powers AS, Reiner A. The distribution of cholinergic neurons in the central nervous system of turtles. Brain Behav Evol 1993;41:326–345. [PubMed: 8324620]

Puelles L, Kuwana E, Puelles E, Bulfone A, Shimamura K, Keleher J, Smiga S, Rubenstein JL. Pallial and subpallial derivatives in the embryonic chick and mouse telencephalon, traced by the expression of the genes Dlx-2, Emx-1, Nkx-2.1, Pax-6, and Tbr-1. J Comp Neurol 2000;424:409–438. [PubMed: 10906711]

Reiner A, Bruce L, Butler A, Csillag A, Kuenzel W, Medina L, Paxinos G, Perkel D, Shimizu T, Striedter G, Wild M, Ball G, Durand S, Gunturkun O, Lee D, Mello CV, Powers A, White S, Hough G, Kubikova L, Smulders TV, Wada K, Dugas-Ford J, Husband S, Yamamoto K, Yu J, Siang C, Jarvis ED. Revised nomenclature for avian telencephalon and some related brainstem nuclei. J Comp Neurol. submitted

Reiner A, Davis BM, Brecha NC, Karten HJ. The distribution of enkephalin-like immunoreactivity in the telencephalon of the adult and developing domestic chicken. J Comp Neurol 1984a;228:245–262. [PubMed: 6207214]

Reiner, A.; Karle, EJ.; Anderson, KD.; Medina, L. Catecholaminergic perikarya and fibers in the avian nervous system. In: Smeets, WJ.; Reiner, A., editors. Phylogeny and development of catecholamine systems in the CNS of vertebrates. Cambridge: Cambridge University Press; 1994. p. 135-181.

Reiner A, Krause JE, Keyser KT, Eldred WD, McKelvy JF. The distribution of substance P in turtle nervous system: A radioimmunoassay and immunohistochemical study. J Comp Neurol 1984b; 226:50–75. [PubMed: 6203942]

Reiner A, Northcutt RG. An immunohistochemical study of the telencephalon of the senegal bichir *Polypterus senegalus*. J Comp Neurol 1992;319:359–386. [PubMed: 1351063]

Reuss S, Hurlbut EC, Speh JC, Moore RY. Neuropeptide Y localization in telencephalic and diencephalic structures of the ground squirrel brain. Am J Anat 1990;188:163–174. [PubMed: 2375281]

Risold PY, Swanson LW. Chemoarchitecture of the rat lateral septal nucleus. Brain Res Brain Res Rev 1997a;24:91–113. [PubMed: 9385453]

Risold PY, Swanson LW. Connections of the rat lateral septal complex. Brain Res Rev 1997b;24:115–195. [PubMed: 9385454]

Roberts TF, Hall WS, Brauth SE. Organization of the avian basal forebrain: chemical anatomy in the parrot (*Melopsittacus undulatus*). J Comp Neurol 2002;454:383–408. [PubMed: 12455005]

Russchen FT, Smeets WJ, Hoogland PV. Histochemical identification of pallidal and striatal structures in the lizard *Gekko gecko*: Evidence for compartmentalization. J Comp Neurol 1987;256:329–341. [PubMed: 2437160]

Sakanaka M, Magari S, Emson PC, Hillyard CJ, Girgis SI, MacIntyre I, Tohyama M. The calcitonin gene-related peptide-containing fiber projection from the hypothalamus to the lateral septal area including its fine structures. Brain Res 1985;344:196–199. [PubMed: 3899279]

Sakanaka M, Magari S, Shibasaki T, Lederis K. Corticotropin releasing factor-containing afferents to the lateral septum of the rat brain. J Comp Neurol 1988;270:404–415. 396–407. [PubMed: 3259589]

Saldanha CJ, Deviche PJ, Silver R. Increased VIP and decreased GnRH expression in photorefractory dark-eyed juncos (*Junco hyemalis*). Gen Comp Endocrinol 1994;93:128–136. [PubMed: 8138113]

Salom S, Font C, Martinez-Garcia F. Seasonal sexually dimorphic distribution of neuropeptide Y-like immunoreactive neurons in the forebrain of the lizard *Podarcis hispanica*. J Chem Neuroanat 1994;7:217–225. [PubMed: 7873094]

Sanchez-Camacho C, Pena JJ, Gonzalez A. Catecholaminergic innervation of the septum in the frog: A combined immunohistochemical and tract-tracing study. J Comp Neurol 2003;455:310–323. [PubMed: 12483684]

Silveira PF, Breno MC, Puorto G, Martin del Rio MP, Mancera JM. Corticotropin-releasing hormone-like immunoreactivity in the brain of the snake *Bothrops jararaca*. Histochem J 2001;33:685–694. [PubMed: 12197677]

Simerly RB, Chang C, Muramatsu M, Swanson LW. Distribution of androgen and estrogen receptor mRNA-containing cells in the rat brain: an in situ hybridization study. J Comp Neurol 1990;294:76–95. [PubMed: 2324335]

Sims KB, Hoffman DL, Said SI, Zimmerman EA. Vasoactive intestinal polypeptide (VIP) in mouse and rat brain: an immunocytochemical study. Brain Res 1980;186:165–183. [PubMed: 6986955]

Smeets WJAJ, Sevensma JJ, Jonker AJ. Comparative analysis of vasotocin-like immunoreactivity in the brain of the turtle *Pseudemys scripta elegans* and the snake *Python regius*. Brain Behav Evol 1990;35:65–84. [PubMed: 2191754]

Stoll CJ, Voorn P. The distribution of hypothalamic and extrahypothalamic vasotocinergic cells and fibers in the brain of a lizard *Gekko gecko* presence of a sex difference. J Comp Neurol 1985;239:193–204. [PubMed: 4044934]

Swanson LW, Sawchenko PE, Rivier J, Vale WW. Organization of ovine corticotropin-releasing factor immunoreactive cells and fibers in the rat brain: an immunohistochemical study. Neuroendocrinology 1983;36:165–186. [PubMed: 6601247]

Szeidemann Z, Shanabrough M, Leranth C. Hypothalamic leu-enkephalin-immunoreactive fibers terminate on calbindin-containing somatospiny cells in the lateral septal area of the rat. J Comp Neurol 1995;358:573–583. [PubMed: 7593751]

Talbot K, Woolf NJ, Butcher LL. Feline islands of Calleja complex: II. Cholinergic and cholinesterasic features. J Comp Neurol 1988;275:580–603. [PubMed: 3192758]

Teruyama R, Beck MM. Double immunocytochemistry of vasoactive intestinal peptide and cGnRH-I in male quail: photoperiodic effects. Cell Tissue Res 2001;303:403–414. [PubMed: 11320656]

Tuinhof R, Gonzalez A, Smeets WJ, Roubos EW. Neuropeptide Y in the developing and adult brain of the South African clawed toad *Xenopus laevis*. J Chem Neuroanat 1994;7:271–283. [PubMed: 7873097]

van Gils J, Absil P, Grauwels L, Moons L, Vandesande F, Balthazart J. Distribution of luteinizing hormone-releasing hormones I and II (LHRH-I and -II) in the quail and chicken brain as demonstrated with antibodies directed against synthetic peptides. J Comp Neurol 1993;334:304–323. [PubMed: 8366198]

Vecino E, Pinuela C, Arevalo R, Lara J, Alonso JR, Aijon J. Distribution of enkephalin-like immunoreactivity in the central nervous system of the rainbow trout: An immunocytochemical study. J Anat 1992;180:435–453. [PubMed: 1487437]

Vecino E, Sharma SC. The development of substance P-like immunoreactivity in the goldfish brain. Anat Embryol 1992;186:41–47. [PubMed: 1381158]

Voorhuis TAM, De Kloet ER. Immunoreactive vasotocin in the zebra finch brain *Taeniopygia guttata*. Dev Brain Res 1992;69:1–10. [PubMed: 1424081]

Voorhuis TAM, Kiss JZ, De Kloet ER, De Wied D. Testosterone-sensitive vasotocin-immunoreactive cells and fibers in the canary brain. Brain Res 1988;442:139–146. [PubMed: 3359249]

Wang R, Millam JR. Corticotropin-releasing hormone-immunopositive nerve elements in apposition to chicken gonadotropin-releasing hormone I-containing perikarya in Japanese quail (*Coturnix coturnix japonica*) brain. Cell Tissue Res 1999;297(2):223–228. [PubMed: 10470492]

Wang Z, Zhou L, Hulihan TJ, Insel TR. Immunoreactivity of central vasopressin and oxytocin pathways in microtine rodents: a quantitative comparative study. J Comp Neurol 1996;366:726–737. [PubMed: 8833119]

Wang ZX, Toloczko D, Young LJ, Moody K, Newman JD, Insel TR. Vasopressin in the forebrain of common marmosets (*Callithrix jacchus*): Studies with in situ hybridization, immunocytochemistry and receptor autoradiography. Brain Res 1997;768:147–156. [PubMed: 9369311]

Watson JT, Adkins-Regan E. Neuroanatomical localization of sex steroid-concentrating cells in the Japanese quail (*Coturnix japonica*): Autoradiography with [3H]-testosterone, [3H]-estradiol, and [3H]-dihydrotestosterone. Neuroendocrinology 1989;49:51–64. [PubMed: 2716950]

Westhoff G, Roth G. Morphology and projection pattern of medial and dorsal pallial neurons in the frog *Discoglossus pictus* and the salamander *Plethodon jordani*. J Comp Neurol 2002;445:97–121. [PubMed: 11891656]

Wong CJH. Connections of the basal forebrain of the weakly electric fish, *Eigenmannia virescens*. J Comp Neurol 1997;389:49–64. [PubMed: 9390759]

Woodhams PL, Roberts GW, Polak JM, Crow TJ. Distribution of neuropeptides in the limbic system of the rat: The bed nucleus of the stria terminalis, septum and preoptic area. Neuroscience 1983;8:677–703. [PubMed: 6346134]

Zupanc GKH, Horschke I, Lovejoy DA. Corticotropin releasing factor in the brain of the gymnotiform fish, *Apteronotus leptorhynchus*: Immunohistochemical studies combined with neuronal tract tracing. Gen Comp Endocrinol 1999;114:349–364. [PubMed: 10336823]

## Abbreviations

**AC**
anterior commissure

**AH**
anterior hypothalamus

**AVT**
arginine vasotocin

**AVP**
arginine vasopressin

**BSTm**
medial bed nucleus of the stria terminalis

**BSTl**
lateral bed nucleus of the stria terminalis

**CcS**
caudocentral septum

**ChAT**
choline acetyltransferase

**CGRP**
calcitonin gene-related peptide

**CoS**
commissural septal nucleus

**CRF**
corticotropin releasing factor

**DBB**
diagonal band of Broca

**ENK**
enkephalin

**GAL**
galanin

**Hp**
hippocampus

**LSr**
lateral septum, rostral division

**LSr.dl**

| | |
|---|---|
| | dorsolateral zone of the LSr |
| **LSr.m** | |
| | medial zone of the LSr |
| **LSc** | |
| | lateral septum, caudal division |
| **LSc.d** | |
| | dorsal zone of the LSc |
| **LSc.l** | |
| | lateral zone of the LSc |
| **LSc.v** | |
| | ventral zone of the LSc |
| **LSc.vl** | |
| | ventrolateral zone of the LSc |
| **LSO** | |
| | lateral septum organ |
| **M** | |
| | mesopallium (“ventral hyperstriatum”)[1] |
| **MS** | |
| | medial septum |
| **MSib** | |
| | internal band of the medial septum |
| **MSt** | |
| | medial striatum (“parolfactory lobe”) [1] |
| **N** | |
| | neopallium (“neostriatum”) [1] |
| **nPC** | |
| | nucleus of the pallial commissure |
| **NPY** | |
| | neuropeptide Y |
| **OM** | |
| | occipitomesencephalic tract |
| **PC** | |
| | pallial commissure |
| **POM** | |
| | medial preoptic nucleus |
| **PVN** | |
| | paraventricular nucleus of the hypothalamus |

[1]Revised nomenclature for the avian telencephalon (Reiner et al., submitted); old nomenclature is given in parentheses

**SFi** septofimbrial nucleus (mammalian)

**SH** septohippocampal septum

**SP** substance P

**TH** tyrosine hydroxylase

**TrSM** septomesencephalic tract

**v** ventricle

**VFI** ventral forebrain island

**VIP** vasoactive intestinal polypeptide

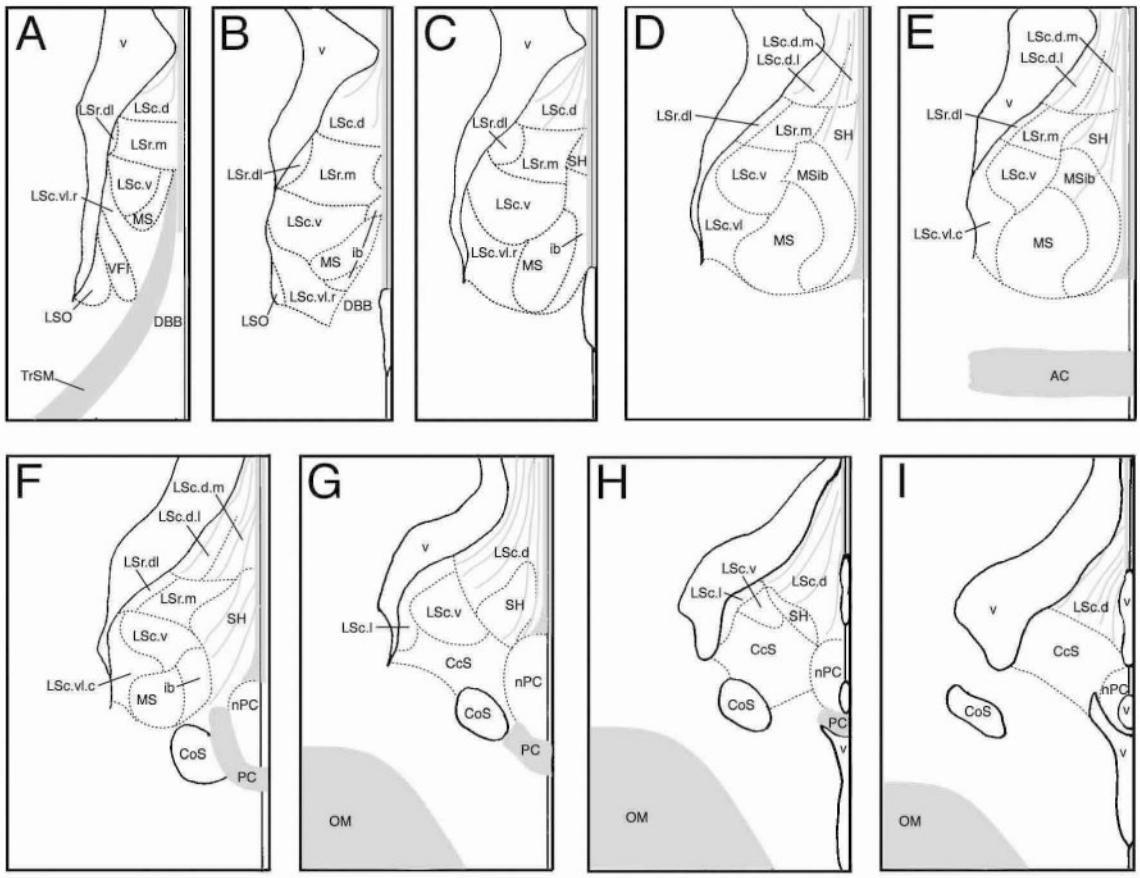


**Figure 1.**

Zones of the songbird septum from rostral **(A)** to caudal **(I)** levels. Zones are based upon the distributions of immunoreactive neuropeptides and enzymes as shown in Table 1. Gray denotes fiber bundles and tracts. The distance between levels is ~200 μm for finches and waxbills.

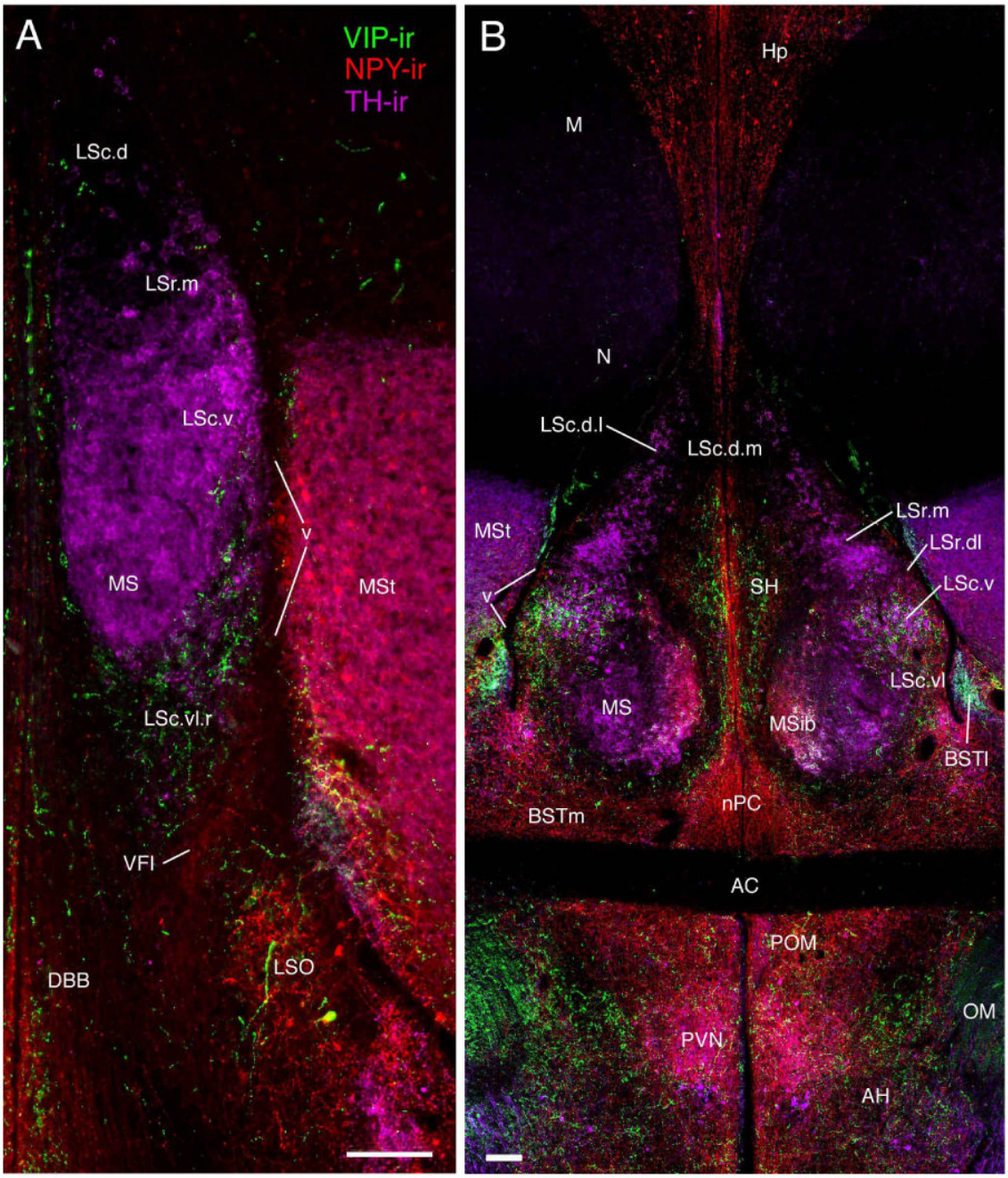


**Figure 2.**
Septal zones at rostral **(A)** and commissural **(B)** levels (corresponding to the approximate levels of Fig. 1A and E, respectively) as demonstrated by triple-labeling of NPY-, TH-, and VIP-ir fibers in a female zebra finch. Scale bars = 100 μm.

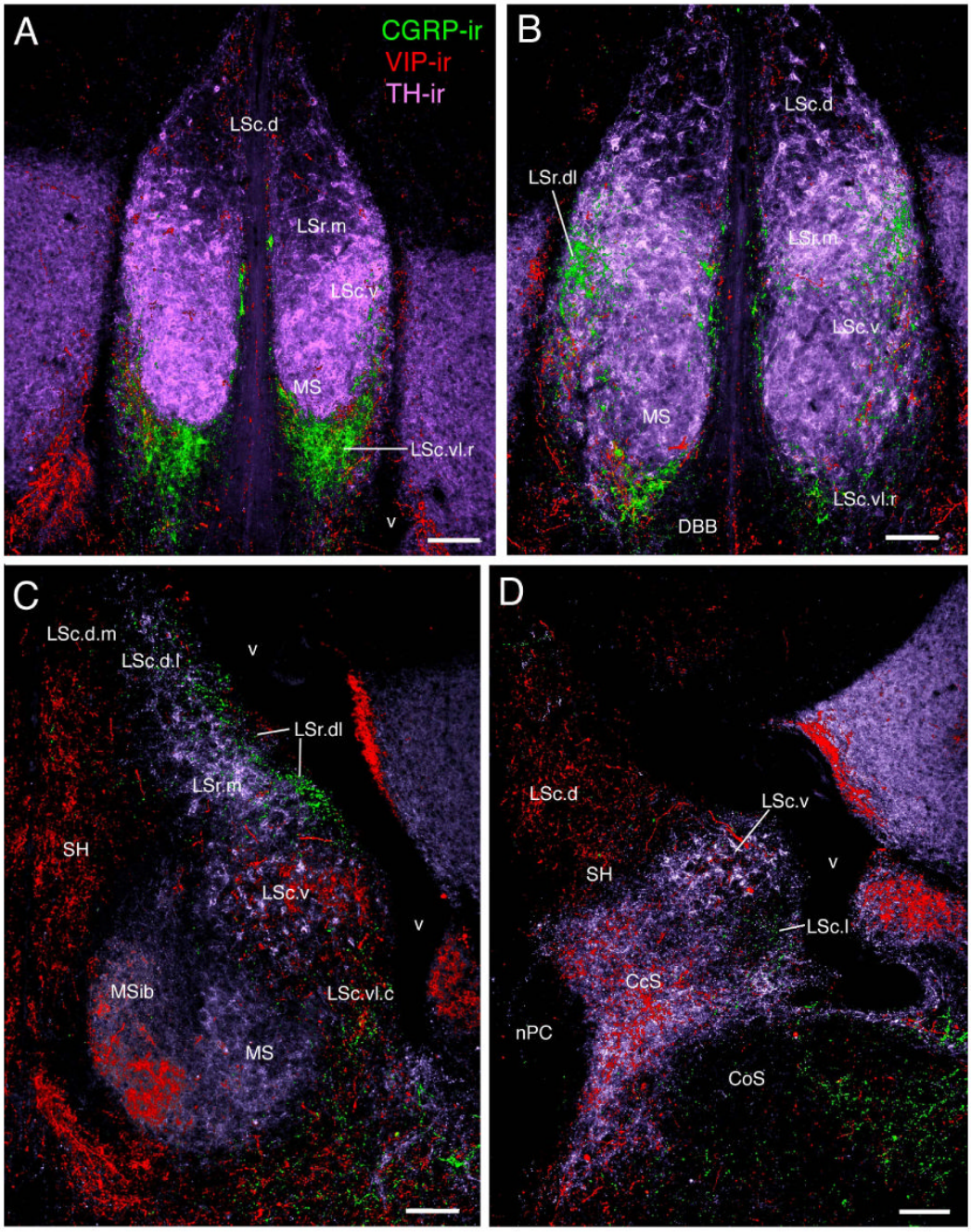


**Figure 3.**

Septal zones as demonstrated by triple-labeling of CGRP-, TH-, and VIP-ir fibers in a female zebra finch. **A)** Photo corresponds to a level intermediate to that depicted in Fig. 1A and B. **B-D)** Photomicrographs at the approximate levels of Fig. 1C, D, and H, respectively. Scale bars = 100 μm.

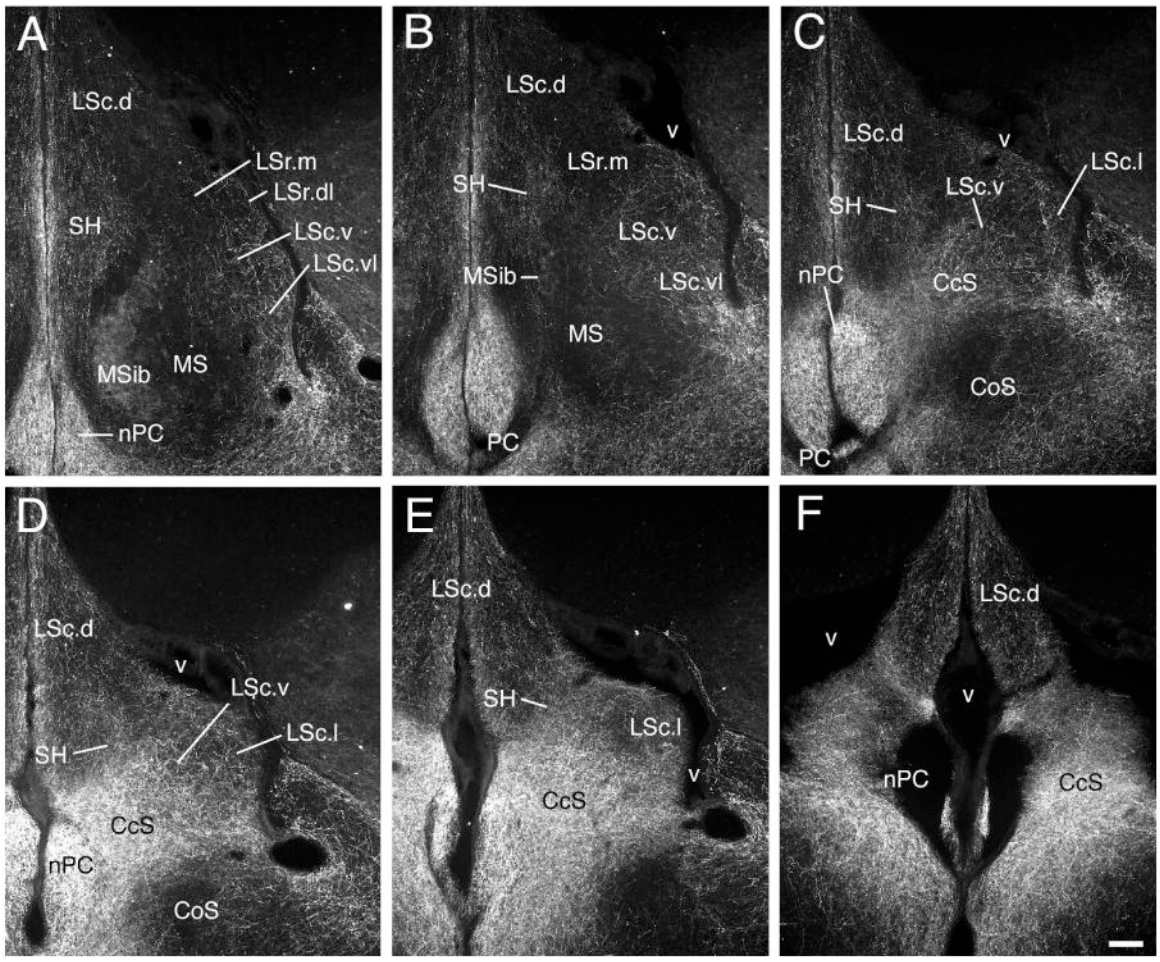


**Figure 4.**

NPY-ir fiber distributions in the zones of the caudal septum in a female zebra finch. Panels **A-F** are a rostrocaudal series (corresponding to the approximate levels of Fig. 1E-I) beginning at commissural levels **(A)**. The MS/MSib shift ventromedially **(A-B)** and disappear as the LSc.vl extends medially **(B)** and the CcS forms **(C).** Concomitantly, the SH moves away from the midline **(B-C)** and begins to flatten across the dorsal margin of the CcS **(D-E)**. Scale bars = 100 μm.

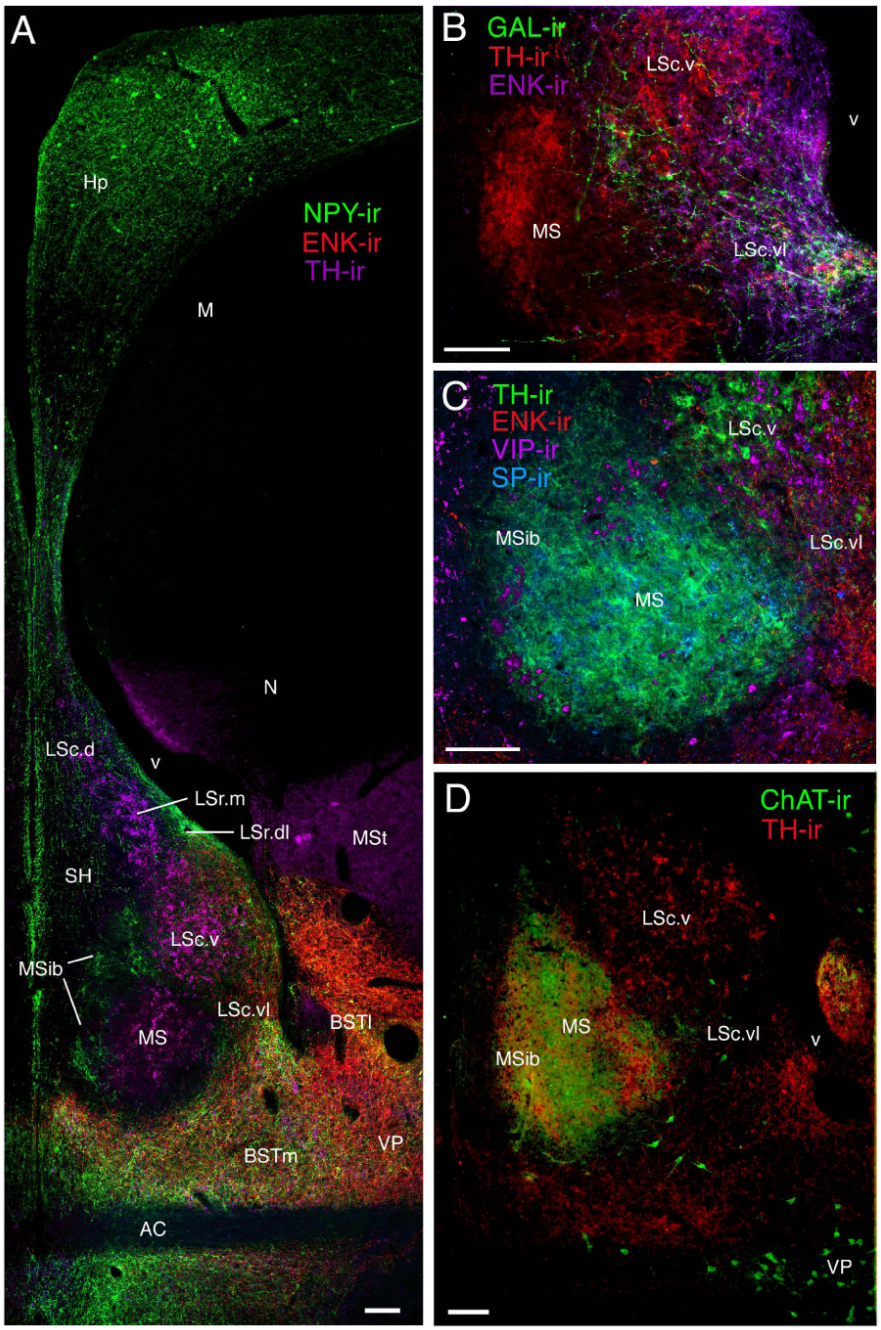


**Figure 5.**

Septal zones at the level of the anterior commissure (approximate level of Fig. 1 E) as demonstrated by multi-labeling of **A)** NPY-, ENK-, and TH-ir fibers, **B)** GAL-, TH-, and ENK-ir fibers, **C)** TH-, ENK-, VIP-, and SP-ir fibers, and **D)** ChAT- and TH-ir fibers. Panels **A and B** are slightly rostral to **C and D**. TH-ir fibers do not enter the MSib at rostral levels of the commissure, but expand into the MSib at caudal levels **(C-D)**. Photos **A-C** are from female zebra finches; **D** is from a male spice finch. Scale bars = 100 μm.

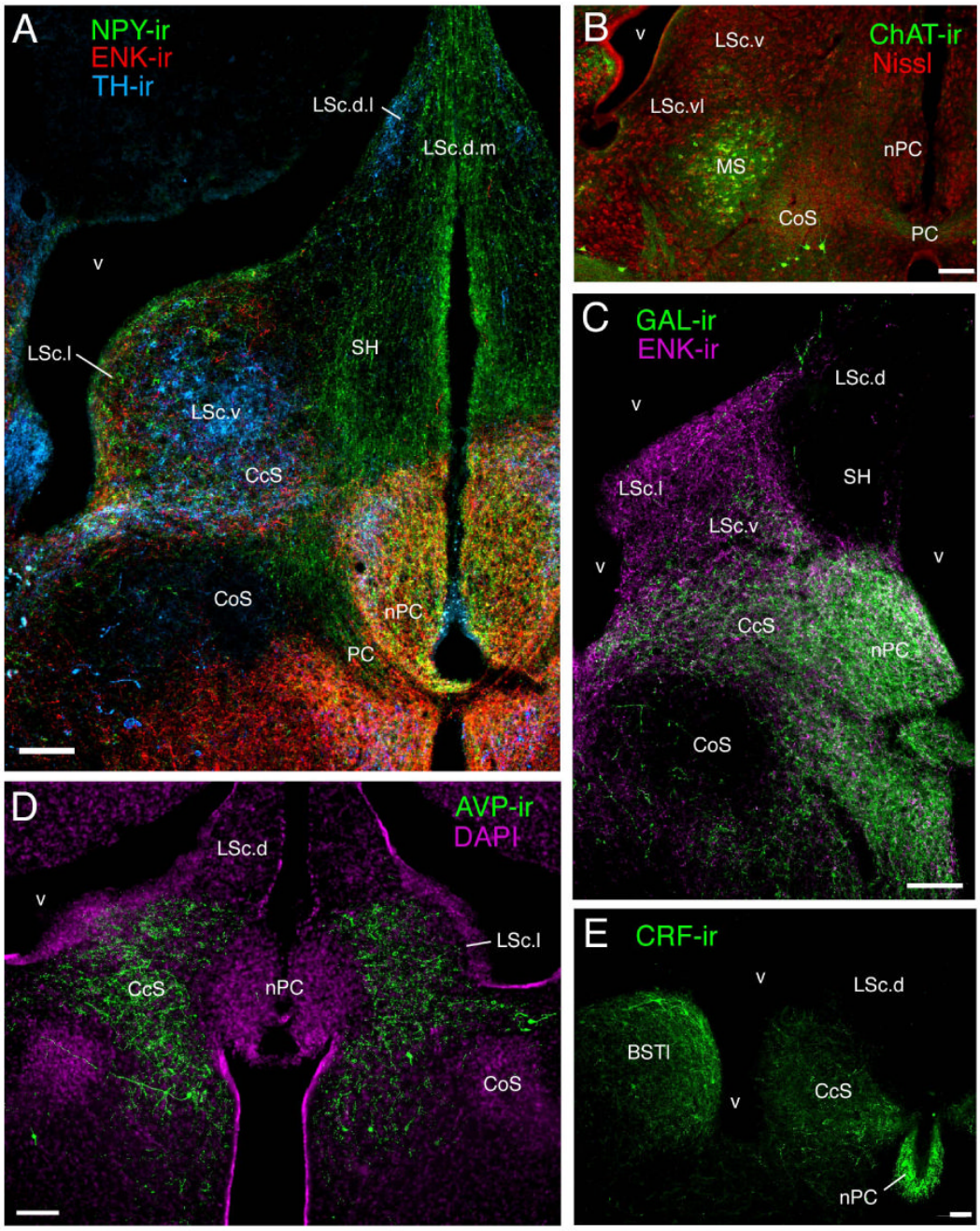


**Figure 6.**

Septal zones at post-commissural levels as demonstrated by labeling of **A)** NPY-, ENK-, and TH-ir fibers in a female zebra finch, corresponding to the level of Fig. 1G, **B)** ChAT-ir neurons in a male spice finch, corresponding to the approximate level of Fig. 1F, **C)** GAL- and ENK -ir fibers in a female zebra finch, corresponding to the level of Fig. 1G, **D)** AVP-ir fibers in a male Angolan blue waxbill, corresponding to a level intermediate to Fig. 1H and I, and **E)** CRF-ir fibers in a male song sparrow, corresponding to the level of Fig. 1I. Scale bars = 100 μm.

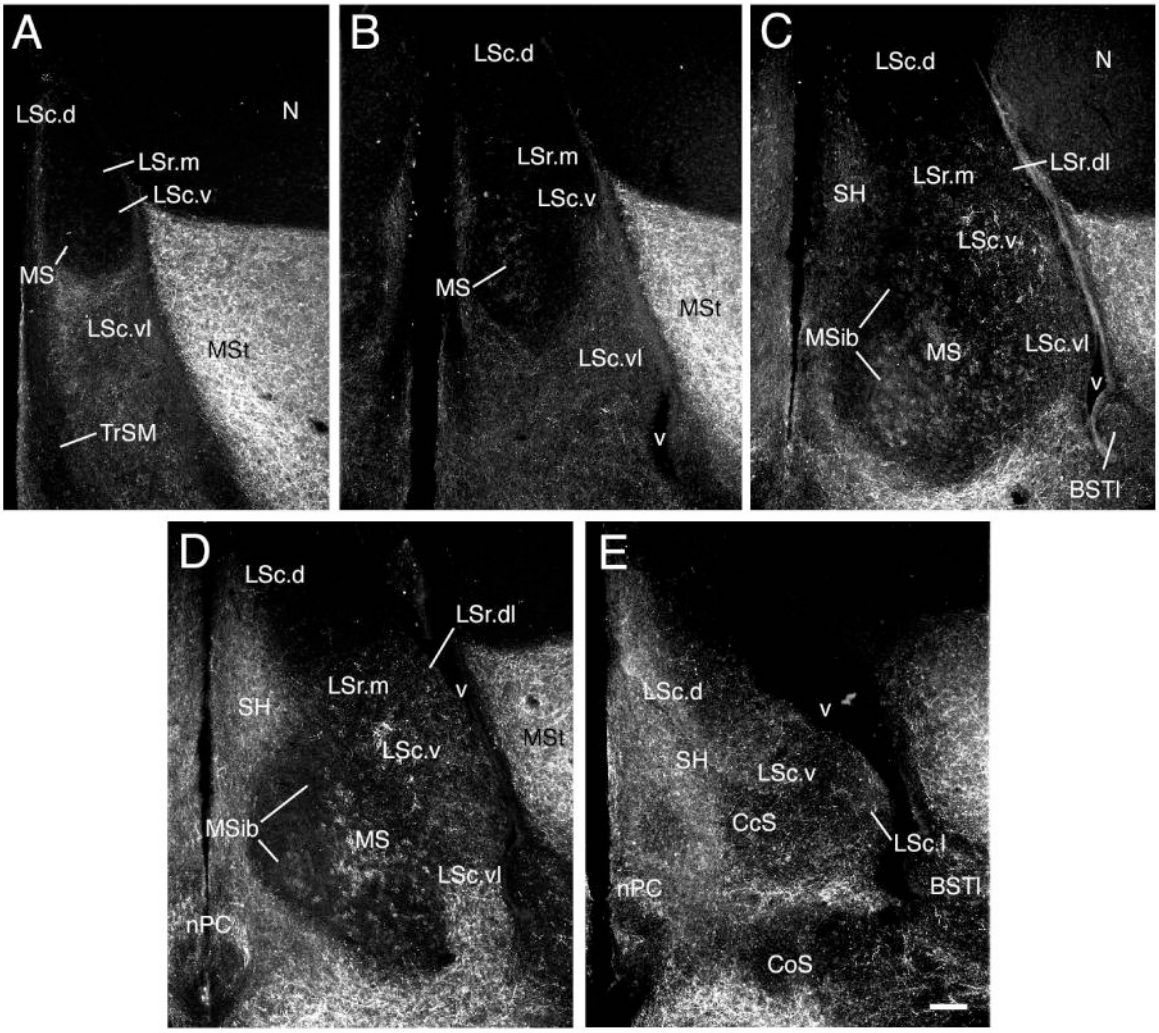


**Figure 7.**

SP-ir fiber distributions in the septum of a male zebra finch. Panels **A-E** are a rostrocaudal series corresponding to the approximate levels of Fig. 1A, B, D/E, F and G, respectively. As shown, SP-ir fibers are widespread in the septum, but exhibit regional differences in density, caliber, varicosity and nesting that clearly define numerous zones. Scale bars = 100 μm.

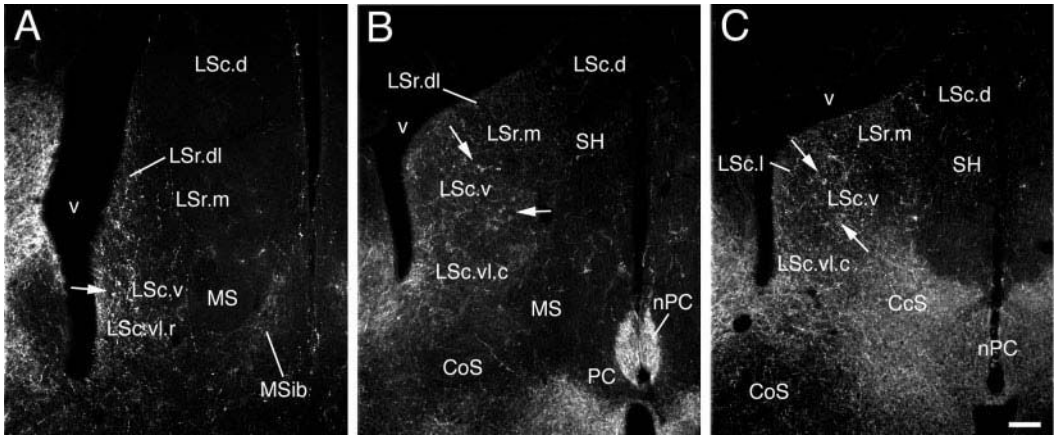


**Figure 8.**
ENK-ir fibers in the septum of a male song sparrow. Panels **A-C** correspond to the approximate levels of Fig. 1C, F, and G/H. Arrows show the locations of pericellular nests in the LSc.v. Scale bars = 100 μm.

**TABLE 1**

Divisions of the songbird septum and proposed mammal equivalents as suggested by immunoreactive terminal fields

| Subdivision | | | | | | | | | | | | | Proposed rat Equivalent[1] |
|---|---|---|---|---|---|---|---|---|---|---|---|---|---|
| part | zone | region | SP | TH | VIP | NPY | AVT | CRF | CGRP | ENK | GAL | ChAT | |
| CcS | | | ++ | +++ | +++ | +++ | +++ | +++ | | +++ | +++ | | SFi? |
| LSc | d | m | +[2] | | +[3] | ++ | | | | | + | | c.d |
| | | l | +[2] | ++ | | ++ | | | + | | + | | c.d.l |
| | l | | ++ | | ++ | +++ | | ++ | | +++ | | | r.dl.l.v? |
| | v | | ++ | +++ | +++ | ++ | + | | | ++ | ++ | | c.v.m |
| | vl | r | ++ | + | ++ | +++ | + | | +++ | +++ | ++ | + | r.dl.m, r.vl.v and c.v.l, in part |
| | | c | ++ | + | +++ | ++ | +++ | + | + | +++ | +++ | + | c.v.l and LSv, in part |
| LSr | dl | | ++ | + | + | +++ | + | | ++ | +++ | + | | r.dl.l |
| | m | | + | +++ | | + | | | | + | + | | r.m |
| MS | | | ++ | +++ | + | + | | | | | + | ++ | MS |
| MSib | | | + | ++[2] | ++ | +++ | | | | + | + | ++ | ? |
| SH | | | ++ | | ++ | +++ | | | | + | | | SH |

[1] Based on divisions of Risold and Swanson, 1997a,b

[2] Absent rostrally

[3] Dense at level of CcS